ChiS is a noncanonical DNA-binding hybrid sensor kinase that directly regulates the chitin utilization program in *Vibrio cholerae*

Catherine A. Klancher[1], Shouji Yamamoto[2], Triana N. Dalia[1], and Ankur B. Dalia[1,*]

[1]Department of Biology, Indiana University, Bloomington, IN 47405
[2]Department of Bacteriology I, National Institute of Infectious Diseases, Tokyo, Japan
*Author for correspondence: ankdalia@indiana.edu

Keywords
Signal transduction, Transcriptional Regulation, Vibrio cholerae

Abstract
Two-component signal transduction systems (TCSs) represent a major mechanism that bacteria use to sense and respond to their environment. Prototypical TCSs are composed of a membrane-embedded histidine kinase (HK), which senses an environmental stimulus and subsequently phosphorylates a cognate partner protein called a response regulator (RR) that regulates gene expression in a phosphorylation-dependent manner. *Vibrio cholerae* uses the hybrid HK ChiS to activate the expression of the chitin utilization program, which is critical for the survival of this facultative pathogen in its aquatic reservoir. A cognate RR for ChiS has not been identified and the mechanism of ChiS-dependent signal transduction remains unclear. Here, we show that ChiS is a noncanonical membrane-embedded one-component system that can both sense chitin and directly regulate gene expression via a cryptic DNA binding domain. Unlike prototypical TCSs, we find that ChiS DNA binding is diminished, rather than stimulated, by phosphorylation. Finally, we provide evidence that ChiS likely activates gene expression by directly recruiting RNA polymerase. Together, this work addresses the mechanism of action for a major transcription factor in *V. cholerae* and highlights the versatility of signal transduction systems in bacterial species.

Significance Statement
From bacteria to humans, the ability to properly respond to environmental cues is critical for survival. The cholera pathogen *Vibrio cholerae* uses one protein, ChiS, to sense chitin in its environmental reservoir to regulate the expression of genes that are critical for the survival and evolution of this pathogen in this niche. Here, we study how the chitin sensor ChiS works, and discover that it regulates gene expression in an unexpected and unorthodox manner. Thus, this study uncovers how the major regulator ChiS works in this important human pathogen and highlights the versatile mechanisms that living systems use to respond to their environment.

Introduction
Vibrio cholerae, the bacterium responsible for the diarrheal disease cholera, is naturally found in the marine environment where it forms biofilms on the chitinous shells of crustacean zooplankton (1). Chitin is a major nutrient source for *V. cholerae* in this niche. In addition to serving as a nutrient source, chitin is also used as a cue to induce horizontal gene transfer by natural transformation. Furthermore, the formation of chitin biofilms promotes the waterborne transmission of cholera in endemic areas (2, 3). Thus, *V. cholerae*-chitin interactions are critical for the survival, evolution, and transmission of this pathogen.

V. cholerae senses chitin via the hybrid sensor kinase ChiS to activate the expression of the chitin utilization program (4, 5). Hybrid sensor kinases are a member of the two-component system (TCS) family of proteins. Prototypical TCSs consist of a membrane-embedded histidine kinase (HK) and a cytoplasmic partner protein called a response regulator (RR) (6). In response to an environmental stimulus, the HK autophosphorylates a conserved histidine. This phosphate is then transferred to a conserved aspartate on the receiver (Rec) domain of its cognate RR. The output activity of the RR, which is DNA-binding in prototypical systems, is enhanced upon

phosphorylation. This leads to altered gene expression is response to the upstream cue sensed by the HK. Hybrid sensor kinases, like ChiS, contain additional domains (Rec and/or histidine phosphotransfer domains) that increase the number of steps in the phosphorelay that leads to phosphorylation of their cognate RR. ChiS contains both HK and Rec domains, including their conserved phosphorylation sites (H469 and D772, respectively) (**Fig. S1**). Though it was discovered ~15 years ago that chitin induces the chitin utilization program of *Vibrio cholerae* through the hybrid HK ChiS, the mechanism of action for this regulator has remained unclear. Here, we show that ChiS does not have a cognate RR, but rather acts as a one-component system that can both sense chitin and directly regulate gene expression from the membrane.

Results

Phosphorylation of the ChiS receiver domain inhibits P_{chb} activation

ChiS is required for activation of the chitin utilization program. To study ChiS activity, we focused on the expression of one activated locus in this genetic program, the *chb* operon (P_{chb}) (7). This operon is responsible for the uptake and degradation of the disaccharide of chitin, chitobiose. In the absence of chitin, ChiS activity is repressed by periplasmic chitin binding protein (CBP) (**Fig. 1a**). It is hypothesized that CBP binding to chitin oligosaccharides relieves this repression and allows ChiS to activate the chitin utilization program. ChiS can also be activated in the absence of chitin oligosaccharides by deletion of *cbp* (**Fig. 1a**). ChiS-dependent regulation of P_{chb} is critical for *V. cholerae* activation of P_{chb} (**Fig. 1a**) and growth on chitobiose (**Fig. 1b**).

To regulate gene expression in response to an environmental stimulus, HKs initiate a phosphorylation cascade via kinase activity to communicate with their cognate RR. Thus, we tested whether the kinase activity and/or phosphorylation of ChiS are required for P_{chb} activation. Mutation of either or both phosphorylation sites in ChiS ($ChiS^{H469A}$, $ChiS^{D772A}$, and $ChiS^{H469A\ D772A}$) still allowed for P_{chb} activation (**Fig. 1a**), and growth on chitobiose (**Fig. S2**), suggesting that the kinase activity and phosphorylation of ChiS are both dispensable, consistent with prior results (8). It is also possible that ChiS may naturally lack kinase activity. To test this, we purified the cytoplasmic domain of ChiS and found that ChiS was, in fact, capable of autophosphorylation *in vitro*, and that this activity was dependent on the conserved histidine in the HK domain (**Fig. S3**).

In addition to autokinase and phosphotransfer activity, HKs also harbor phosphatase activity. In some HKs, a conserved threonine is critical for phosphatase activity, but is dispensable for kinase activity (9, 10). This residue is conserved in ChiS (**Fig. S1**), and when mutated ($ChiS^{T473A}$), we observed a loss of P_{chb}-GFP activation and slightly delayed growth on chitobiose (**Fig. 1**), while growth on other carbon sources was unaffected (**Fig. S4**). Importantly, all ChiS alleles were expressed at similar levels *in vivo* (**Fig. S5**). Also, $ChiS^{T473A}$ still exhibited kinase activity *in vitro*, albeit at a reduced level compared to the parent (**Fig. S3**). These results suggested that ChiS phosphatase activity is critical for P_{chb} activation. Demonstrating ChiS phosphatase activity *in vitro* is challenging because there are two sites of phosphorylation on the same protein. Thus, we took a genetic approach to test whether $ChiS^{T473A}$ was a poor activator of P_{chb} due to a loss of phosphatase activity.

If ChiS^{T473A} is phosphatase inactive, this would result in constitutive phosphorylation of the conserved aspartate in the ChiS Rec domain, which may inactivate ChiS and result in decreased P_{chb} expression. Therefore, we hypothesized that preventing phosphorylation of the ChiS Rec domain should recover P_{chb} activation, even in the ChiS phosphatase inactive background. To test this, we prevented phosphorylation of this ChiS Rec domain in the ChiS^{T473A} background by either mutating the phosphorylated aspartate (ChiS$^{T473A\ D772A}$) or by preventing ChiS kinase activity (ChiS$^{T473A\ H469A}$). Both mutants rescued P_{chb} activation (**Fig. 1**) and growth on chitobiose (**Fig. S2d-e**), suggesting that the ChiS^{T473A} mutation prevents activation of P_{chb} due to constitutive phosphorylation of the ChiS Rec domain. To further test whether phosphorylation of the Rec domain prevents activation of P_{chb}, we generated a phosphomimetic allele by mutating the conserved aspartate to a glutamate (11) (ChiS^{D772E}). We found that ChiS^{D772E} did not activate P_{chb} and markedly slowed growth on chitobiose (**Fig. 1**). The effect of ChiS^{D772E} on growth was much stronger than for ChiS^{T473A}, likely because ChiS^{T473A} may still have low levels of unphosphorylated ChiS, while the phosphomimetic mutation in ChiS^{D772E} ensures that all copies of ChiS resemble the phosphorylated form.

Collectively, these data suggest that phosphorylation of the ChiS Rec domain prevents its activity, while de-phosphorylation of the Rec domain activates ChiS. Additionally, these data demonstrate that CBP does not repress ChiS by regulating its kinase/phosphatase activity because ChiS mutants that are constitutively unphosphorylated (e.g. ChiS$^{H469A\ D772A}$) still require inactivation of *cbp* to induce ChiS activity (**Fig. 1a**).

ChiS is a one-component membrane-bound phosphorylation-dependent DNA binding protein

ChiS is a hybrid HK and it was presumed to regulate gene expression in conjunction with a cognate RR tentatively named ChiR (5). However, no candidate for ChiR has ever been identified despite numerous attempts from our group and others (4, 5, 7). Additionally, ChiS is active when its kinase activity is ablated, making it unlikely that this HK passes a phosphate to a cognate RR. This led us to hypothesize that ChiS directly regulates gene expression in response to chitin.

To test this, we assessed whether ChiS was sufficient to activate a P_{chb}-*lacZ* reporter in the heterologous host *Escherichia coli*, which lacks a ChiS homolog. Similar to what we observe in *V. cholerae*, ChiS induced P_{chb} expression in *E. coli* and this activity was diminished in the phosphomimetic ChiS^{D772E} background (**Fig. 2a**). Together, these data suggest that ChiS directly activates P_{chb}.

We hypothesized that ChiS directly regulates P_{chb} by binding to the promoter. To test this, we generated a functional internally FLAG-tagged ChiS (**Fig. S5**) and performed ChIP-qPCR to see if this protein bound to the *chb* promoter *in vivo*. When ChiS is active (ChiS-FLAG^{WT} Δ*cbp*), P_{chb} was enriched ~70-fold, suggesting that ChiS directly binds P_{chb} *in vivo* (**Fig. 2b**). Enrichment of P_{chb} was also observed in the heterologous host *E. coli* (**Fig. 2a**). When ChiS activity is repressed due to the presence of CBP in *V.*

cholerae, we find that ChiS binding to P_{chb} is significantly reduced, suggesting that CBP may antagonize ChiS by preventing its DNA binding activity (**Fig. 2b**).

The DNA-binding activity of prototypical RRs is controlled by the phosphorylation status of the conserved aspartate in their Rec domain. To determine whether the phosphorylation status of ChiS Rec plays a role in regulating DNA-binding, ChIP assays were performed with the phosphomimetic ChiS-FLAG^{D772E}. We observed that ChIP enrichment and P_{chb} expression were significantly decreased (**Fig. 2b**), suggesting that phosphorylation of the Rec domain decreases the affinity of ChiS for DNA, which results in loss of *chb* expression.

The phosphorylation state of RRs, however, generally only alters their affinity for DNA and not their absolute ability to bind DNA. Consistent with this, overexpression of ChiS-FLAG^{D772E} resulted in ChIP enrichment similar to the ChiS parent (**Fig. 2b**). Additionally, overexpression of ChiS-FLAG^{D772E} partially restored P_{chb} expression (**Fig. 2b**), suggesting that reduced activation by this phosphomimetic allele is largely attributed to its reduced affinity for DNA.

ChiS has two predicted transmembrane (TM) domains. Based on the domain architecture, we predicted that the sequence between the two TM domains would be periplasmic, and the sequence following the second TM would be cytoplasmic (predicted topology in **Fig. S6a**). We tested the membrane topology of ChiS using *lacZ* and *phoA* fusions, which rely on the observation that LacZ is only functional in the cytoplasm and PhoA is only functional in the periplasm (12-14). The LacZ fusions tested exhibited high activity only when linked to a residue before the first TM (ChiS$^{1-2}$), or past the second TM (ChiS$^{1-452}$ and ChiS$^{1-1129}$; **Fig. S6b**). Conversely, the only PhoA fusion that was functional was linked to a residue between the first and second TMs (ChiS$^{1-52}$; **Fig. S6b**). These data were consistent with the predicted membrane topology (**Fig. S6a**).

Typically, DNA-binding transcription factors are soluble cytoplasmic proteins. It is possible that ChiS is proteolytically processed to release a cytoplasmic DNA-binding portion of the protein, or it is possible that ChiS directly binds to DNA from the membrane. If ChiS is post-translationally processed, we hypothesized that P_{chb} should only be enriched during ChIP experiments when the FLAG tag in ChiS is cytoplasmically-localized, and not when the FLAG tag is periplasmically-localized because the latter should be separated from the cytoplasmic DNA-binding domain following proteolytic cleavage. To test this, we generated two functional alleles of ChiS where the FLAG tag was inserted in the cytoplasmic domain (after residue E566; see **Fig. S6a**) or the periplasmic domain (after residue T287; see **Fig. S6a**). We observed similar levels of P_{chb} enrichment in both strains (**Fig. 2b**), indicating that ChiS likely binds P_{chb} from the membrane *in vivo*.

Specific binding of ChiS to P_{chb} is required for activation of the chb operon
Thus far, we have shown that ChiS binds to P_{chb} *in vivo* via ChIP assays. This assay relies on crosslinking to stabilize protein-DNA interactions, and it remained possible that

the enrichment we observed was not due to ChiS directly binding P_{chb}, but instead was the result of ChiS being in a complex with a crosslinked partner protein (like an RR) that binds to DNA. To further test whether ChiS binds DNA directly or indirectly, we purified a fragment of ChiS encompassing the Rec domain and C-terminus ($ChiS^{Rec-C}$) and tested its ability to bind P_{chb} via electrophoretic mobility shift assays (EMSAs) *in vitro*. We found that purified $ChiS^{Rec-C}$ binds to a P_{chb} DNA probe. This interaction could be competed with unlabeled P_{chb}, but not an unrelated promoter, demonstrating that this interaction is both direct and specific (**Fig. S7**). Next, we sought to narrow down the location of the ChiS binding site(s) within the *chb* promoter. Through EMSA analysis of P_{chb} promoter fragments (**Fig. S8**), we identified two distinct 13bp sequences that represented two putative ChiS binding sites (CBSs).

To test these putative CBSs, a 60bp probe that spans both sites (**Fig. S9**) was used for EMSA analysis (**Fig. 3a**). When ChiS was incubated with the WT probe, we observed three shifts. Two of these shifts are likely due to the two CBSs in this probe, while the third shift may result from DNA bending as described for other transcriptional regulators (15, 16). Mutation of either CBS in isolation results in loss of one shift, while mutation of both CBSs completely prevents ChiS binding (**Fig. 3a**). Additionally, ChiS does not bind to a full length P_{chb} probe when both CBSs are mutated, confirming that these are the only two CBSs within this promoter (**Fig. S7**). Furthermore, use of the CBS 1 & 2 mutated P_{chb} probe as a cold competitor does not prevent ChiS binding to WT P_{chb} (**Fig. S7**). Finally, the CBSs are conserved within P_{chb} in diverse *Vibrio* species (**Fig. S10a**).

To characterize the role of the CBSs in P_{chb} activation and *V. cholerae* physiology, we mutated these sites in the P_{chb}-GFP reporter and at the native locus, respectively. Mutation of either CBS significantly decreased P_{chb} expression (**Fig. 3c**) and correspondingly slightly delayed growth on chitobiose (**Fig. 3b**). However, mutation of both CBSs completely prevents P_{chb} activation and growth on chitobiose (**Fig. 3b-c**). Collectively, these data indicate that ChiS binding to the *chb* promoter is required for activation.

Our *in vivo* and *in vitro* data showing that ChiS directly binds P_{chb} was unexpected because ChiS lacks a canonical DNA binding domain based on primary sequence (BLAST (17)) or structural homology (Phyre2 (18)) predictions. We hypothesized that the C-terminal 197 amino acids of ChiS (residues 937-1129; see **Fig. S6**), which have no predicted homology to other domains and are conserved among ChiS homologs (**Fig. S10b**), encoded a noncanonical DNA binding domain. To test this, we performed ChIP experiments with N-terminal truncations of ChiS, which revealed that the C-terminal 106 amino acids of ChiS were sufficient to bind P_{chb} *in vivo* (**Fig. S9**). Further, deletion of these residues from full length ChiS prevented P_{chb} enrichment (**Fig. S9**), indicating that this domain is necessary and sufficient for DNA binding. These experiments also revealed that while cytoplasmic fragments of ChiS were sufficient to bind P_{chb} *in vivo*, they did not activate P_{chb} expression (**Fig. S9**).

ChiS may activate P_{chb} by direct recruitment of the alpha subunit of RNAP

Finally, we sought to define the mechanism by which ChiS activates gene expression. Some activators promote transcription by directly recruiting RNA Polymerase (RNAP). Previous work with activators like CRP, shows that the absolute distance between the activator binding site and promoter is not critical for activation, but the phasing of DNA between these sites is critical to ensure that the transcription factor recruits RNAP in the correct orientation (19, 20). One turn of B DNA is 10bp; thus, insertions or deletions of 10bp should maintain helical phasing, while insertions or deletions of 5bp should ablate phase-dependent interactions.

To assess if CBSs needed to be in phase with the *chb* promoter to mediate activation of P_{chb}, we inserted 5 or 10 bp between the CBSs and the -35 signal (**Fig. 4a, Region A**). Insertion of 5bp, which would put the CBSs and -35 out of phase, resulted in loss of P_{chb} expression; insertion of 10bp, which maintains helical phasing, allowed for partial activation (**Fig. 4a-b**). A distance-dependent reduction in transcriptional activation despite maintenance of phase-dependent interactions is consistent with prior results in other regulators (20). These results suggest that CBSs must be in phase with the -35 to activate P_{chb}.

In addition to ChiS, other DNA binding proteins, like SlmA, bind upstream of the CBSs and contribute to P_{chb} activation (7). To assess if upstream factors exhibit helical phase-dependence for P_{chb} activation, we inserted or deleted 5 or 10 bp upstream of the CBSs (**Fig. 4a, Region B**). We found that indels of 5bp (loss of helical phasing) resulted in loss of P_{chb} expression, while indels of 10bp (helical phasing maintained) allowed for partial activation (**Fig. 4a-b**). This suggests that factors upstream of the CBSs must be in phase for proper activation of P_{chb}.

Collectively, these data support either of the following models for proper P_{chb} activation: 1) CBSs and other upstream activator binding sites must all be in phase with the -35, or 2) only upstream activator binding sites need to be in phase with the -35 while the CBSs do not. To distinguish between these two models, we introduced mutations to isolate the phasing of the CBSs. When 5bp is inserted at Region A, both the CBSs and the upstream activator binding sites are out of phase. We restored helical phasing for the upstream activator binding sites, but not the CBSs, by inserting or deleting 5bp from Region B. We observed that P_{chb} activation is not restored when phasing is restored for the upstream activator binding sites, which suggests that both the CBSs and upstream activator sites must be in phase with the -35 signal for activation of P_{chb}. The spacing between the CBSs and the -35 signal in P_{chb} is conserved across *Vibrio* species (**Fig. S10a**), further indicating an important role for DNA phasing in activation of *chb* expression.

Helical phase dependence between the CBSs and the -35 supports a model where ChiS directly recruits RNAP. Transcriptional activators that recruit RNAP often interact with the α-subunit, and so we hypothesized that ChiS may directly interact with RpoA. To test this, we assessed directing binding between purified $ChiS^{cytoplasmic}$ and RpoA *in vitro* using a protein pulldown assay. In pulldown reactions where RpoA was the prey,

RpoA only came out in the elution when ChiS^{cytoplasmic} was used as the bait, suggesting that ChiS and α-subunit interact (**Fig. 4**). Reciprocal pulldowns using RpoA as the bait further confirmed this interaction (**Fig. S11**).

Discussion

TCSs represent a diverse family of proteins that allow bacteria to sense and respond to their environment. Here, we describe a protein that, based on homology, falls into the two-component family, but uses a mechanism that is contrary to the canon for these systems. ChiS is noncanonical in two ways (**Fig. 5**). First, phosphorylation of the Rec domain diminishes its output activity while dephosphorylation enhances it. To our knowledge, this is the first example of such regulation among TCS family proteins. Second, ChiS is able to bind P_{chb} from the membrane to regulate gene expression. This result was particularly surprising because ChiS lacks a canonical DNA-binding domain.

It is tempting to speculate that the ChiS C-terminus represents a novel class of DNA-binding domain. Homology searches (BLAST) revealed that this DNA-binding domain is exclusively found at the C-terminus of other proteins (**Fig. S12**), which often contain an N-terminal sensing domain (i.e. HK/Rec or PAS (6, 21, 22)). This analysis also revealed that this domain is largely restricted to gamma- and deltaproteobacteria, with a few examples among alphaproteobacteria. This suggests that this DNA-binding domain may not be unique to *V. cholerae* ChiS, but may be a conserved output domain for diverse signal transduction proteins in proteobacteria.

ChiS activity is regulated by the physiology of the cell at multiple levels (**Fig. 5**). In the absence of chitin, CBP inhibits ChiS DNA-binding activity (**Fig. 5a**). ChiS activity is also negatively regulated by carbon catabolite repression (CCR) (23), suggesting that the chitin utilization program is suppressed in the presence of preferred carbon sources. The mechanism underlying CCR-dependent inhibition of ChiS, however, remains unclear and will be the focus of future work. It is also possible that additional cues regulate ChiS activity. For example, it remains unclear what role ChiS kinase/phosphatase activity plays in regulating this system because CBP-dependent repression ensures that ChiS activity is suppressed in the absence of chitin. It is possible that additional currently unknown factors regulate ChiS kinase/phosphatase activity (**Fig. 5b**). ChiS has a C-terminal PAS domain (**Fig. S6a**) which may modulate ChiS enzymatic activities as described for other HKs (24, 25). The complex regulation of ChiS activity may act to integrate additional cues that ultimately control expression of the chitin utilization program.

Hybrid HKs that putatively bind DNA are uncommon, but not unprecedented. *Bacteroides thetaiotaomicron* encodes 33 hybrid HKs, 32 of which contain AraC-type DNA binding domains within their C-terminus (26). However, these proteins have merely been identified by bioinformatic analyses and, to our knowledge, the molecular mechanism of DNA-binding HKs has not previously been tested in any system. Here, we show that ChiS is a one-component hybrid HK that directly binds DNA from the membrane to regulate gene expression. Aside from TCSs, membrane-embedded DNA-

binding transcriptional regulators are conserved in bacterial species, with ChiS representing the fourth such member within *V. cholerae* (alongside ToxR, TcpP, and TfoS (8, 27-30)). We show that ectopic expression of just the cytoplasmic domain of ChiS is sufficient to bind DNA *in vivo*, but does not activate gene expression (**Fig. S9**). Thus, it is tempting to speculate that the capacity of membrane-embedded regulators to recruit target promoters to the cell periphery is critical for their ability to activate transcription (31). Also, the mechanism by which membrane-embedded regulators access their target sites in the genome while being sequestered in the membrane remains poorly understood (32). ChiS may serve as a valuable model system to dissect the molecular mechanism of membrane-embedded regulators, which will be the focus of future work.

Methods

Bacterial strains and culture conditions

All *V. cholerae* strains used in this study are derived from the El Tor strain E7946 (33). The *E. coli* strains used to test ChiS activity in a heterologous host were derived from MG1655 (34), while the strains used to test ChiS membrane topology were derived from *E. coli* DH1 (35). *V. cholerae* and *E. coli* strains were grown in LB medium and on LB agar supplemented when necessary with carbenicillin (20 or 100 µg/mL), kanamycin (50 µg/mL), spectinomycin (200 µg/mL), trimethoprim (10 µg/mL), and/or chloramphenicol (2 µg/mL).

Generating Mutant Strains

V. cholerae mutant constructs were generated using splicing-by-overlap extension exactly as previously described (36). See **Table S3** for all of the primers used to generate mutant constructs in this study. Mutant *V. cholerae* strains were generated by chitin-dependent natural transformation and cotransformation exactly as previously described (37, 38).

The P_{chb}-*lacZ* reporter was introduced into *E. coli* MG1655 using λ Red recombineering (39). *E. coli* MG1655 harboring pKD46 was subcultured in SOB medium supplemented with 100 µg/mL carbenicillin and 0.02% arabinose at 30°C until an OD_{600} of 0.6 was reached. Cells were washed with ice cold 10% glycerol, electroporated with 200 ng Kan^R-P_{chb} PCR product (amplified using primers described in **Table S3**), outgrown in SOC medium for 1 hour at 37°C, then plated on selective media.

Mutant strains were confirmed by PCR and/or sequencing. See **Table S2** for a detailed list of mutant strains used in this study.

Plasmid Construction

Plasmids for protein purification and the Miller assays to test ChiS activity in **Fig. 2** were constructed using the FastCloning method (40). Vectors and inserts were amplified using the primers listed in **Table S3**. Plasmids used for the Miller assays to define ChiS membrane topology in **Fig. S6** were made by cloning amplified inserts into the SalI and XbaI sites of pMW-SY*lacZ* or pMW-SY*phoA*.

Measuring GFP Fluorescence
GFP fluorescence was determined essentially as previously described (7, 41). Briefly, single colonies were picked and grown in LB broth at 30°C for 18 hours. Cells were then washed and resuspended to an OD_{600} of 1.0 in instant ocean medium (7g/L; Aquarium Systems). Then, GFP fluorescence was determined using a BioTek H1M plate reader with excitation set to 500 nm and emission set to 540 nm.

Growth Curves
Growth was kinetically monitored at 30°C with shaking using a BioTek H1M plate reader with absorbance set to 600 nm. Growth was tested using M9 minimal medium supplemented with the indicated carbon source to a final concentration of 0.2%. *V. cholerae* can grow on chitobiose through both the activity of the chitobiose ABC transporter encoded within the *chb* operon and through a GlcNAc PTS transporter (7, 42). ChiS is only required for regulation of the chitobiose ABC transporter (7). Thus, to study the effect of ChiS on regulating chitobiose utilization, the PTS GlcNAc transporter VC0995 was inactivated in all strains used to test growth as previously described (7).

Miller Assay
To assess ChiS activity in MG1655 strains, overnight cultures were inoculated from single colonies and grown at 30°C for 18 hours in LB broth supplemented with carbenicillin (100 µg/mL), kanamycin (50 µg/mL), and IPTG (10 µM). LacZ activity was then determined exactly as previously described (43).

For membrane topology experiments, overnight cultures of strains grown at 37°C in LB broth supplemented with ampicillin (100 µg/mL) were subcultured 1:50 into fresh LB broth containing ampicillin (100 µg/mL) and grown with shaking at 37°C for 2.5 hours to an OD_{600} of ~0.7-1.0. Cells were then harvested, and alkaline phosphatase (PhoA) and beta-galactosidase (LacZ) activities of strains (as appropriate) were determined as previously described (44, 45).

Chromatin Immunoprecipitation (ChIP) Assay
Overnight cultures of strains for ChIP were diluted to an OD_{600} of 0.08 and then grown for 6 hours at 30°C with rolling. For strains with natively expressed ChiS, cells were grown in plain LB broth. For *V. cholerae* strains containing P_{tac} constructs, cells were grown in LB broth supplemented with IPTG (10 µM). For *E. coli* strains, cells were grown in LB broth supplemented with kanamycin (50 µg/mL), carbenicillin (100 µg/mL), and IPTG (10 µM). Cultures were crosslinked with paraformaldehyde (1% final concentration) for 20 minutes at room temperature, quenched with Tris for 10 minutes at room temperature, washed twice with TBS (25 mM Tris HCl pH 7.5 and 125 mM NaCl), and then cell pellets were stored at -80°C overnight. Cell pellets were resuspended to an OD_{600} of 50 in Lysis Buffer (1x FastBreak cell lysis reagent (Promega), 50 µg/mL lysozyme, 1% Triton X-100, 1 mM PMSF, and 1x protease inhibitor cocktail; 100x inhibitor cocktail contained the following: 0.07 mg/mL phosphoramidon (Santa Cruz), 0.006 mg/mL bestatin (MPbiomedicals/Fisher Scientific), 1.67 mg/mL AEBSF (DOT Scientific), 0.07 mg/mL pepstatin A (Gold Bio), 0.07 mg/mL E64 (Gold Bio)). Cells were lysed with a QSonica Q55 tip probe sonicator, resulting in a DNA shear size of ~500 bp.

Lysates were clarified by centrifugation and then diluted 5-fold in IP Buffer (50 mM HEPES NaOH pH 7.5, 150 mM NaCl, 1 mM EDTA, and 1% Triton X-100). Diluted lysates were applied to Anti-FLAG M2 Magnetic Beads (Sigma) equilibrated in IP buffer. Lysates were incubated with beads at room temperature with end-over-end mixing for 2 hours. Beads were then washed twice with IP Buffer, once with Wash Buffer 1 (50 mM HEPES NaOH pH 7.5, 1 mM EDTA, 1% Triton X-100, 500 mM NaCl, and 0.1% SDS), once with Wash Buffer 2 (10 mM Tris HCl pH 8.0, 250 mM LiCl, 1 mM EDTA, 0.5% NP-40, and 1% Triton X-100), and finally once with TE (10 mM tris pH 8.0 and 1 mM EDTA). Bound protein-DNA complexes were eluted off the beads by incubation with Elution Buffer (50 mM Tris HCl pH 7.5, 10 mM EDTA, and 1% SDS) at 65°C for 30 minutes. Samples were digested with 20 µg Proteinase K in Elution Buffer for 2 hours at 42°C, then crosslinks were reversed by incubating samples at 65°C for 6 hours.

DNA samples were cleaned up and used as template for quantitative PCR (qPCR) using iTaq Universal SYBR Green Supermix (Bio-Rad) and primers specific for the genes indicated (primers are listed in **Table S3**) on a Step-One qPCR system. Standard curves of genomic DNA were included in each experiment and were used to determine the abundance of each amplicon in the input (derived from the lysate prior to ChIP) and output (derived from the samples after ChIP). Primers to amplify *rpoB* served as a baseline control in this assay because ChiS does not bind this locus. Data are reported as 'Fold Enrichment', which is defined as the ratio of P_{chb}/*rpoB* DNA found in the output divided by the ratio of P_{chb}/*rpoB* DNA found in the input.

Protein Purification

For purification of $ChiS^{Rec\text{-}C}$ (which contained an N-terminal 6x-histidine tag), *E. coli* BL21 harboring the vector of interest was grown shaking at 37°C in LB supplemented with 100 µg/mL carbenicillin until an OD_{600} of 0.6 was reached. Protein expression was induced by the addition of IPTG to a final concentration of 100 µM, and cells were grown shaking at 30°C for an additional 4 hours. Cell pellets were stored at -80°C overnight. Pellets were resuspended in Buffer A (50 mM Tris HCl pH 7.5, 500 mM NaCl, 1 mM DTT, 20 mM imidazole, and 10% glycerol) supplemented with 2 mg/mL DNaseI, 1 mM PMSF, and 1 mg/mL lysozyme, then incubated rocking at room temperature for 20 minutes. Cells were lysed by French Press, clarified by centrifugation, and then applied to a HisTrap HP Nickel column (GE Healthcare). The column was washed with Buffer A, and then the protein was eluted using a gradient with Buffer B (50 mM Tris HCl pH 7.5, 500 mM NaCl, 1 mM DTT, 500 mM imidazole, and 10% glycerol). Fractions were stored at -80°C in single use aliquots, which were subsequently used for EMSAs.

For purification of MBP-$ChiS^{cytoplasmic}$ isoforms, *E. coli* BL21 harboring the vectors of interest were grown at 37°C with shaking in LB supplemented with 100 µg/mL carbenicillin to an OD_{600} of 0.6. Protein expression was induced by the addition of IPTG to a final concentration of 1 mM and cells were grown shaking at 30°C for an additional 4 hours. Cell pellets were stored at -80°C overnight. Pellets were resuspended in Column Buffer (20 mM Tris HCl pH 8.0, 200 mM NaCl, 1 mM EDTA, and 1 mM DTT) supplemented with 2 mg/L DNaseI, 1 mM PMSF, and 1 mg/mL lysozyme. Lysis reactions were incubated rocking at 4°C for 20 minutes, then cells were lysed by

sonication. Lysates were clarified by centrifugation and then applied to amylose resin (NEB). Resin was washed with 10x column volumes of Column Buffer, and then protein was eluted with Elution Buffer (20 mM Tris HCl pH 8.0, 200 mM NaCl, 1mM EDTA, 1 mM DTT, and 10 mM maltose). Protein was exchanged into Storage Buffer (20 mM tris HCl pH 8.0, 25 mM KCl, 1 mM DTT, 10% glycerol) using PD-10 desalting columns (GE Healthcare). Buffer exchanged protein was stored in aliquots at -80°C.

The α-subunit of RNA Polymerase from *Vibrio harveyi* was purified exactly as previously described(46).

Electrophoretic Mobility Shift Assays
Binding reactions contained 10 mM Tris HCl pH 7.5, 1 mM EDTA, 10 mM KCl, 1 mM DTT, 50 µg/mL BSA, 0.1 mg/mL salmon sperm DNA, 5% glycerol, 1 nM of a Cy5 labeled DNA probe, and $ChiS^{Rec\text{-}C}$ at the indicated concentrations (diluted in 10 mM Tris pH 7.5, 10 mM KCl, 1 mM DTT, and 5% glycerol). Reactions were incubated at room temperature for 20 minutes in the dark, then electrophoretically separated on polyacrylamide gels in 0.5x Tris Borate EDTA (TBE) buffer at 4°C. Gels were imaged for Cy5 fluorescence on a Typhoon-9210 instrument.

Short DNA probes (30-60bp) were made by end-labeling one primer of a complementary pair (primers listed in **Table S3**) using 20 µM Cy5-dCTP and Terminal deoxynucleotidyl Transferase (TdT; Promega). Complementary primers (one labeled with Cy5 and the other unlabeled) were annealed by slow cooling at equimolar concentrations in annealing buffer (10 mM Tris pH 7.5 and 50 mM NaCl). P_{chb} and $P_{VCA0053}$ probes were made by Phusion PCR, where Cy5-dCTP was included in the reaction at a level that would result in incorporation of 1–2 Cy5 labeled nucleotides in the final probe as previously described (36).

Protein Pulldown
Purified 6xHis-α-subunit of RNA Polymerase from *V. harveyi* and purified MBP-$ChiS^{cytoplasmic}$ were incubated in Pulldown Buffer (50 mM HEPES pH 7.5, 200 mM NaCl, 0.1% Triton X-100, 1 mM DTT, and 0.1 mg/mL salmon sperm DNA) at room temperature for 30 minutes. Each protein was present at a final concentration of 2 µM. For reactions using 6xHis-α-subunit as the bait, buffers were supplemented with 13 mM imidazole. For reactions with no bait, the storage buffer for each protein was added at an equal volume as the bait protein. Protein incubation reactions were applied to amylose resin or cobalt resin (pre-equilibrated with Pulldown Buffer) and incubated rocking at room temperature for 30 minutes. After pulldown, the supernatant (FT) was reserved, then beads were washed 5 times with Pulldown Buffer. Bait protein was eluted with 500 mM imidazole (using 6x His-α-subunit as the bait) or 10 mM maltose (using MBP-$ChiS^{cytoplasmic}$ as bait). FT and Elution samples were then subject to Western blot analysis.

Western Blot Analysis
For *in vivo* sample Western blots, strains were grown as described for ChIP assays, pelleted, resuspended, and boiled in 1x SDS PAGE sample buffer (110 mM Tris pH 6.8,

12.5% glycerol, 0.6% SDS, 0.01% Bromophenol Blue, and 2.5% β-mercaptoethanol). For *in vitro* sample Western blots, protein samples were mixed with an equal volume of 2x SDS PAGE sample buffer. Proteins were separated by SDS polyacrylamide gel electrophoresis, then transferred to a PVDF membrane, and probed with rabbit polyconal α-FLAG (Sigma), rabbit polyclonal α-MBP (Sigma), or mouse monoclonal α-RpoA (Biolegend) primary antibodies. Blots were then incubated with α-rabbit or α-mouse secondary antibodies conjugated to IRdye 800CW (Licor) as appropriate and imaged using an Odyssey classic LI-COR imaging system.

In vitro kinase assay
Purified MBP-ChiS^{cytoplasmic} alleles were diluted to 5 μM in kinase buffer (50 mM Tris HCl pH 8.0, 50 mM KCl, 5 mM MgCl2, 1 mM DTT), then kinase reactions were initiated with the addition of 200 μM ATP and 0.125 μCi/μL ATP [γ-^{32}P]. Reactions were incubated at room temperature for 30 minutes, then separated by SDS polyacrylamide gel electrophoresis. Gels were dried, exposed to a Phosphoimager Screen overnight, and then imaged on a Typhoon-9210 instrument.

Statistics
Statistical differences were assessed by one-way ANOVA followed by a multiple comparisons Tukey's post-test using GraphPad Prism software. All means and statistical comparisons can be found in **Table S1.**

Acknowledgements
We would like to thank Mark Goulian, David Grainger, Clay Fuqua, Daniel Kearns, Julia van Kessel, and Malcolm Winkler for helpful discussions. We thank Alyssa Ball and Ryan Chaparian for advice on experimental set up and for supplying reagents for protein pulldown and ChIP experiments. This work was supported by grants R35GM128674 and AI118863 from the National Institutes of Health to ABD and grant no. 19K07551 from JSPS (the Japan Society for the Promotion of Sciences) KAKENHI to SY.

References
1. Pruzzo C, Vezzulli L, & Colwell RR (2008) Global impact of Vibrio cholerae interactions with chitin. *Environ Microbiol* 10(6):1400-1410.
2. Colwell RR*, et al.* (2003) Reduction of cholera in Bangladeshi villages by simple filtration. *Proc Natl Acad Sci U S A* 100(3):1051-1055.
3. Huq A*, et al.* (2010) Simple sari cloth filtration of water is sustainable and continues to protect villagers from cholera in Matlab, Bangladesh. *mBio* 1(1).
4. Li X & Roseman S (2004) The chitinolytic cascade in Vibrios is regulated by chitin oligosaccharides and a two-component chitin catabolic sensor/kinase. *Proc Natl Acad Sci U S A* 101(2):627-631.
5. Meibom KL*, et al.* (2004) The Vibrio cholerae chitin utilization program. *Proc Natl Acad Sci U S A* 101(8):2524-2529.
6. Stock AM, Robinson VL, & Goudreau PN (2000) Two-component signal transduction. *Annu Rev Biochem* 69:183-215.

7. Klancher CA, Hayes CA, & Dalia AB (2017) The nucleoid occlusion protein SlmA is a direct transcriptional activator of chitobiose utilization in Vibrio cholerae. *PLoS Genet* 13(7):e1006877.
8. Yamamoto S*, et al.* (2014) Regulation of natural competence by the orphan two-component system sensor kinase ChiS involves a non-canonical transmembrane regulator in Vibrio cholerae. *Molecular microbiology* 91(2):326-347.
9. Dutta R, Yoshida T, & Inouye M (2000) The critical role of the conserved Thr247 residue in the functioning of the osmosensor EnvZ, a histidine Kinase/Phosphatase, in Escherichia coli. *J Biol Chem* 275(49):38645-38653.
10. Wayne KJ, Li S, Kazmierczak KM, Tsui HC, & Winkler ME (2012) Involvement of WalK (VicK) phosphatase activity in setting WalR (VicR) response regulator phosphorylation level and limiting cross-talk in Streptococcus pneumoniae D39 cells. *Mol Microbiol* 86(3):645-660.
11. Klose KE, Weiss DS, & Kustu S (1993) Glutamate at the site of phosphorylation of nitrogen-regulatory protein NTRC mimics aspartyl-phosphate and activates the protein. *J Mol Biol* 232(1):67-78.
12. Silhavy TJ & Beckwith JR (1985) Uses of lac fusions for the study of biological problems. *Microbiol Rev* 49(4):398-418.
13. Manoil C & Beckwith J (1986) A genetic approach to analyzing membrane protein topology. *Science* 233(4771):1403-1408.
14. Manoil C, Mekalanos JJ, & Beckwith J (1990) Alkaline phosphatase fusions: sensors of subcellular location. *J Bacteriol* 172(2):515-518.
15. Marbaniang CN & Gowrishankar J (2012) Transcriptional cross-regulation between Gram-negative and gram-positive bacteria, demonstrated using ArgP-argO of Escherichia coli and LysG-lysE of Corynebacterium glutamicum. *J Bacteriol* 194(20):5657-5666.
16. Wang L, Helmann JD, & Winans SC (1992) The A. tumefaciens transcriptional activator OccR causes a bend at a target promoter, which is partially relaxed by a plant tumor metabolite. *Cell* 69(4):659-667.
17. Altschul SF, Gish W, Miller W, Myers EW, & Lipman DJ (1990) Basic local alignment search tool. *J Mol Biol* 215(3):403-410.
18. Kelley LA, Mezulis S, Yates CM, Wass MN, & Sternberg MJ (2015) The Phyre2 web portal for protein modeling, prediction and analysis. *Nat Protoc* 10(6):845-858.
19. Gaston K, Bell A, Kolb A, Buc H, & Busby S (1990) Stringent spacing requirements for transcription activation by CRP. *Cell* 62(4):733-743.
20. Ushida C & Aiba H (1990) Helical phase dependent action of CRP: effect of the distance between the CRP site and the -35 region on promoter activity. *Nucleic Acids Res* 18(21):6325-6330.
21. Henry JT & Crosson S (2011) Ligand-binding PAS domains in a genomic, cellular, and structural context. *Annu Rev Microbiol* 65:261-286.
22. Taylor BL & Zhulin IB (1999) PAS domains: internal sensors of oxygen, redox potential, and light. *Microbiol Mol Biol Rev* 63(2):479-506.
23. Yamamoto S & Ohnishi M (2017) Glucose-Specific Enzyme IIA of the Phosphoenolpyruvate:Carbohydrate Phosphotransferase System Modulates Chitin Signaling Pathways in Vibrio cholerae. *J Bacteriol* 199(18).

24. Gutu AD, Wayne KJ, Sham LT, & Winkler ME (2010) Kinetic characterization of the WalRKSpn (VicRK) two-component system of Streptococcus pneumoniae: dependence of WalKSpn (VicK) phosphatase activity on its PAS domain. *J Bacteriol* 192(9):2346-2358.
25. Sobran MA & Cotter PA (2019) The BvgS PAS Domain, an Independent Sensory Perception Module in the Bordetella bronchiseptica BvgAS Phosphorelay. *J Bacteriol* 201(17).
26. Martens EC, Chiang HC, & Gordon JI (2008) Mucosal glycan foraging enhances fitness and transmission of a saccharolytic human gut bacterial symbiont. *Cell Host Microbe* 4(5):447-457.
27. Dalia AB, Lazinski DW, & Camilli A (2014) Identification of a membrane-bound transcriptional regulator that links chitin and natural competence in Vibrio cholerae. *mBio* 5(1):e01028-01013.
28. Miller VL, Taylor RK, & Mekalanos JJ (1987) Cholera toxin transcriptional activator toxR is a transmembrane DNA binding protein. *Cell* 48(2):271-279.
29. Hase CC & Mekalanos JJ (1998) TcpP protein is a positive regulator of virulence gene expression in Vibrio cholerae. *Proc Natl Acad Sci U S A* 95(2):730-734.
30. Krukonis ES, Yu RR, & Dirita VJ (2000) The Vibrio cholerae ToxR/TcpP/ToxT virulence cascade: distinct roles for two membrane-localized transcriptional activators on a single promoter. *Mol Microbiol* 38(1):67-84.
31. Crawford JA, Krukonis ES, & DiRita VJ (2003) Membrane localization of the ToxR winged-helix domain is required for TcpP-mediated virulence gene activation in Vibrio cholerae. *Mol Microbiol* 47(5):1459-1473.
32. Roggiani M & Goulian M (2015) Chromosome-Membrane Interactions in Bacteria. *Annu Rev Genet* 49:115-129.
33. Miller VL, DiRita VJ, & Mekalanos JJ (1989) Identification of toxS, a regulatory gene whose product enhances toxR-mediated activation of the cholera toxin promoter. *J Bacteriol* 171(3):1288-1293.
34. Hayashi K*, et al.* (2006) Highly accurate genome sequences of Escherichia coli K-12 strains MG1655 and W3110. *Mol Syst Biol* 2:2006 0007.
35. Hanahan D (1983) Studies on transformation of Escherichia coli with plasmids. *J Mol Biol* 166(4):557-580.
36. Dalia AB, Lazinski DW, & Camilli A (2013) Characterization of undermethylated sites in Vibrio cholerae. *J Bacteriol* 195(10):2389-2399.
37. Dalia AB, McDonough E, & Camilli A (2014) Multiplex genome editing by natural transformation. *Proc Natl Acad Sci U S A* 111(24):8937-8942.
38. Dalia AB (2018) Natural Cotransformation and Multiplex Genome Editing by Natural Transformation (MuGENT) of Vibrio cholerae. *Methods Mol Biol* 1839:53-64.
39. Datsenko KA & Wanner BL (2000) One-step inactivation of chromosomal genes in Escherichia coli K-12 using PCR products. *Proc Natl Acad Sci U S A* 97(12):6640-6645.
40. Li C*, et al.* (2011) FastCloning: a highly simplified, purification-free, sequence- and ligation-independent PCR cloning method. *BMC Biotechnol* 11:92.
41. Dalia AB (2016) RpoS is required for natural transformation of Vibrio cholerae through regulation of chitinases. *Environ Microbiol* 18(11):3758-3767.

42. Hayes CA, Dalia TN, & Dalia AB (2017) Systematic genetic dissection of PTS in Vibrio cholerae uncovers a novel glucose transporter and a limited role for PTS during infection of a mammalian host. *Molecular microbiology* 104(4):568-579.
43. Nickels BE (2009) Genetic assays to define and characterize protein-protein interactions involved in gene regulation. *Methods* 47(1):53-62.
44. Brickman E & Beckwith J (1975) Analysis of the regulation of Escherichia coli alkaline phosphatase synthesis using deletions and phi80 transducing phages. *J Mol Biol* 96(2):307-316.
45. Miller JH (1972) *Experiments in molecular genetics* (Cold Spring Harbor Laboratory Press, Cold Spring Harbor, NY).
46. Ball AS & van Kessel JC (2019) The master quorum-sensing regulators LuxR/HapR directly interact with the alpha subunit of RNA polymerase to drive transcription activation in Vibrio harveyi and Vibrio cholerae. *Mol Microbiol* 111(5):1317-1334.
47. Grebe TW & Stock JB (1999) The histidine protein kinase superfamily. *Adv Microb Physiol* 41:139-227.
48. Blattner FR*, et al.* (1997) The complete genome sequence of Escherichia coli K-12. *Science* 277(5331):1453-1462.

Figures

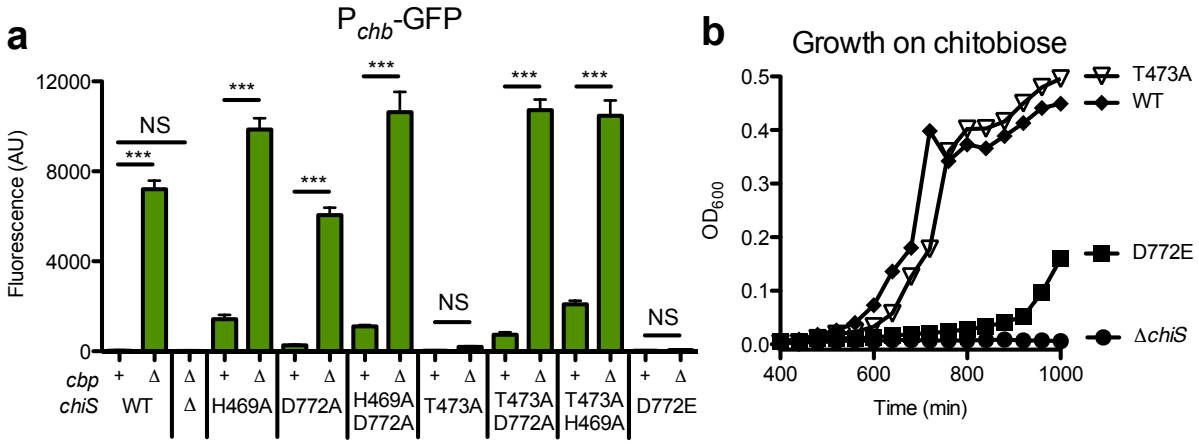

Fig. 1. *Phosphorylation of the ChiS receiver domain inhibits P_{chb} activation*. Point mutants of ChiS in the conserved sites of phosphorylation (H469, D772) or a residue required for phosphatase activity (T473) were assessed for activation of P_{chb} using (**a**) a P_{chb}-GFP transcriptional reporter (ChiS allele genotype indicated on the X-axis) or (**b**) growth on minimal medium containing chitobiose as the sole carbon source. In **a**, strains either have CBP intact (+) or deleted (Δ) as indicated; in **b**, all strains have CBP intact. Data in **a** are from at least three independent biological replicates and shown as the mean ± SD; data in **b** are representative of two independent experiments. Statistical comparisons in **a** were made by one-way ANOVA with Tukey's post-test. NS, not significant. ***, $p < 0.001$. For a detailed list of all statistical comparisons see **Table S1**.

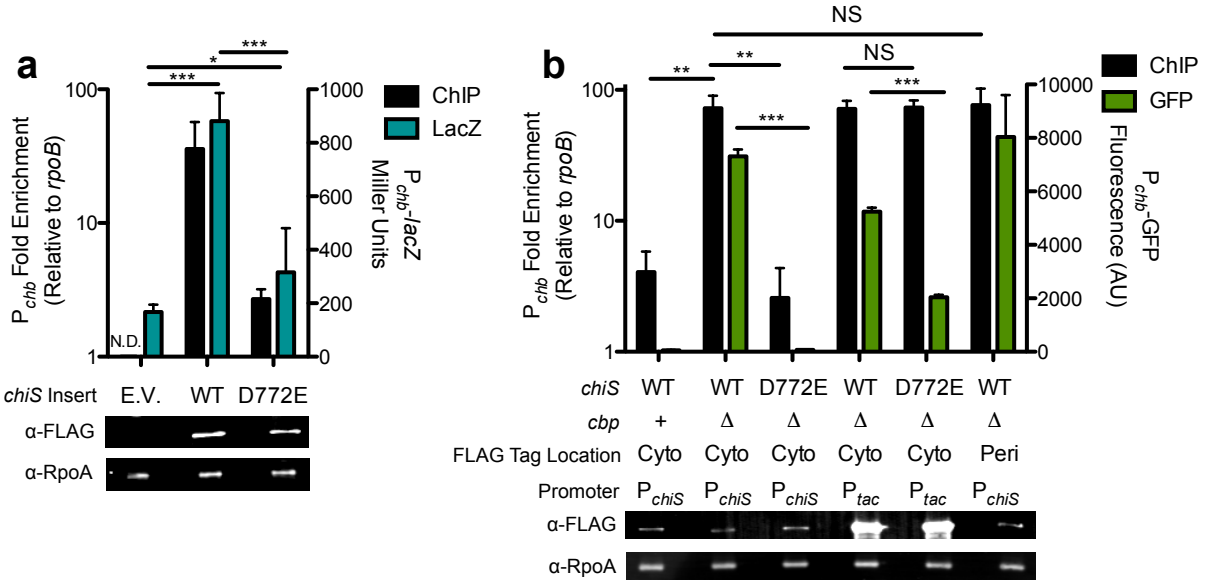

Fig. 2. *ChiS is a one-component membrane-bound phosphorylation-dependent DNA binding protein.* (**a**) Miller assay and chromatin immunoprecipitation (ChIP) performed in *E. coli* MG1655 containing a chromosomally-encoded P_{chb}-*lacZ* reporter and pMMB empty vector (E.V.) or vectors containing the ChiS allele indicated. Untagged ChiS alleles were used for Miller assays (blue bars), while ChiS-FLAG alleles were used for ChIP assays (black bars). P_{chb} enrichment was assessed relative to *rpoB* for ChIP assays. For the empty vector strain, ChIP enrichment was not determined (N.D). (**b**) *V. cholerae* strains expressing ChiS-FLAG alleles under native or P_{tac} overexpression conditions as indicated were assessed for P_{chb} enrichment relative to *rpoB* via ChIP (black bars), activation of a P_{chb}-GFP reporter (green bars), and expression of either ChiS (anti-FLAG) or RpoA (anti-RpoA; loading control) via Western blot analysis. ChiS alleles had a FLAG tag localized to either the cytoplasmic domain (cyto) or the periplasmic (peri) domain of ChiS; ChiS membrane topology is schematized in **Fig S6**. All data are from at least three independent biological replicates and shown as the mean ± SD. Statistical comparisons were made by one-way ANOVA with Tukey's post-test. NS, not significant. *, $p < 0.05$. **, $p < 0.01$. ***, $p < 0.001$.

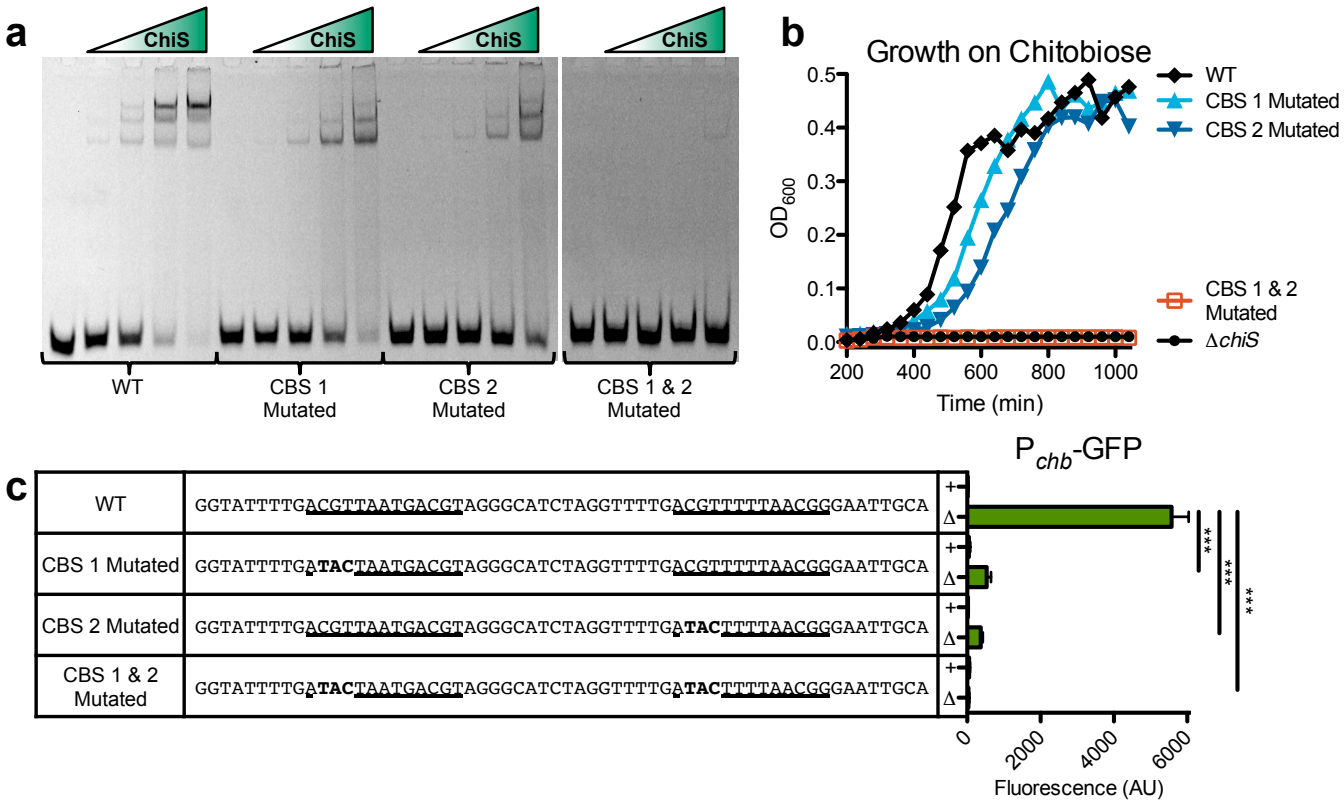

Fig. 3. *Specific binding of ChiS to P_{chb} is required for activation of the chb operon*. (**a**) Electrophoretic mobility shift assays (EMSAs) were carried out using a purified portion of the ChiS cytoplasmic domain ($ChiS^{Rec\text{-}C}$, residues 725-1129 – see **Fig. S6**) and a Cy5-labeled 60 bp fragment of the P_{chb} promoter that is either intact or mutated as indicated (exact sequences in **c**). This 60 bp fragment encompasses both ChiS binding sites (CBSs) (see **Fig. S7**). (**b**) Strains containing the indicated mutations in the native P_{chb} promoter were assessed for growth on chitobiose. Data in **a-b** are representative of at least 2 independent experiments. (**c**) Expression of a P_{chb}-GFP reporter containing the indicated mutations to the ChiS binding sites was assessed in strains where *cbp* is intact (+) or deleted (Δ) as indicated. Data are the result of at least three independent biological replicates and shown as the mean ± SD. Statistical comparisons were made by one-way ANOVA with Tukey's post-test. ***, $p < 0.001$.

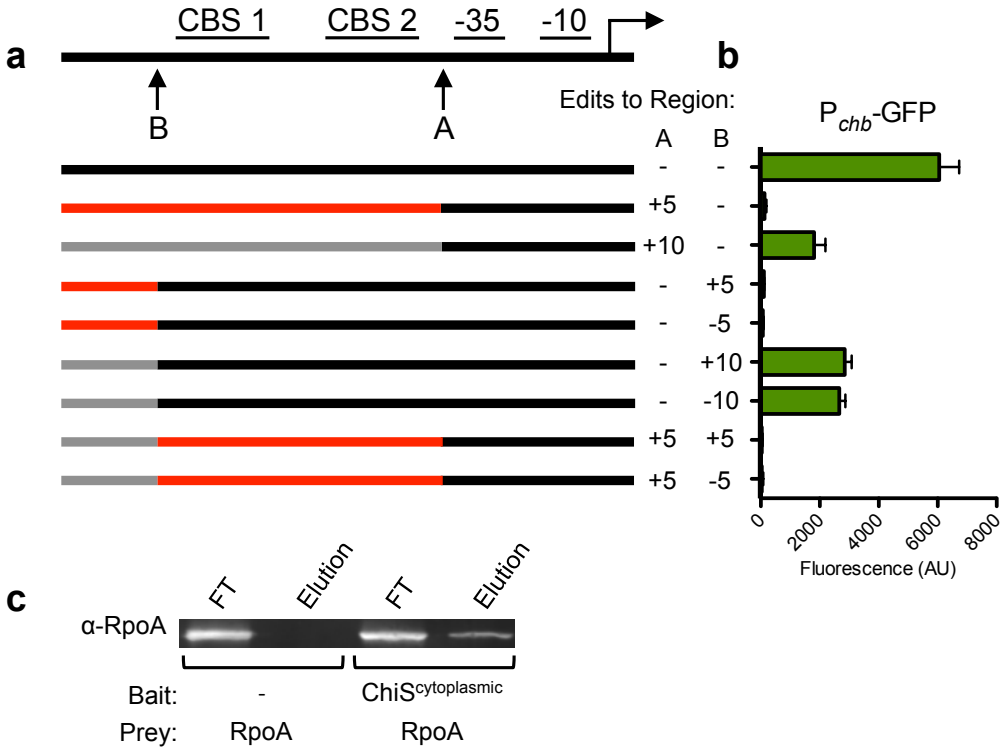

Fig. 4. *ChiS may activate P_{chb} by direct recruitment of the alpha subunit of RNAP.* (**a**) Schematic of the approach to test phase-dependent activation of P_{chb}. Indels of 5 or 10bp were introduced at region A and B to alter the phasing of the elements within P_{chb} relative to the -35 signal. For each mutant generated, the schematic highlights the phasing of promoter elements with respect to the -35. WT phasing is indicated in black, if the sequence is mutated to be out-of-phase it is indicated in red, and if the sequence is mutated to maintain helical phasing it is indicated in gray. (**b**) P_{chb}-GFP expression was determined for strains harboring the indicated phase-mutated P_{chb}-GFP alleles. Data are the result of at least three independent biological replicates and shown as the mean ± SD. (**c**) Protein pulldown assays were performed using purified ChiS (MBP-tagged $ChiS^{cytoplasmic}$) as bait and purified RpoA as prey as indicated. The presence of the RpoA prey was assessed in the flow through (FT) and elution by Western blot analysis. Data are representative of two independent experiments.

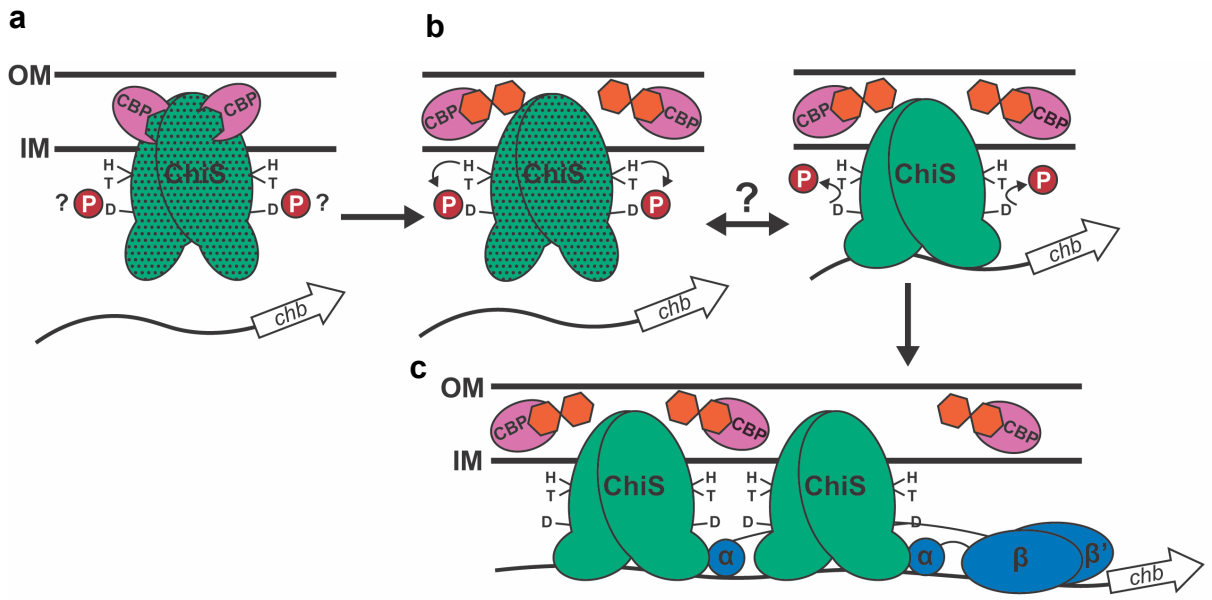

Figure 5. *Proposed model for ChiS-mediated activation of P_{chb}*. (**a**) In the absence of chitin, CBP (pink) is thought to bind to the periplasmic domain of ChiS (green) which prevents activation of P_{chb} by forcing the ChiS DNA-binding domain into a conformationally inactive state (stippled). CBP does not repress ChiS by regulating its kinase/phosphatase activity, and it is unclear what the phosphorylation state of ChiS is in the CBP bound state. (**b**) In the presence of chitin oligomers (orange hexagons), ChiS is no longer repressed by CBP, though other currently unknown cues may play an additional regulatory role in skewing ChiS toward kinase (center) or phosphatase (right) activity. (**c**) Upon a switch to phosphatase activity, ChiS is active and can bind P_{chb} and activate transcription by recruiting RNA polymerase through a direct interaction with the alpha subunit.

Supplemental Information for:

ChiS is a noncanonical DNA-binding hybrid sensor kinase that directly regulates the chitin utilization program in *Vibrio cholerae*

Catherine A. Klancher[1], Shouji Yamamoto[2], Triana N. Dalia[1], and Ankur B. Dalia[1,*]

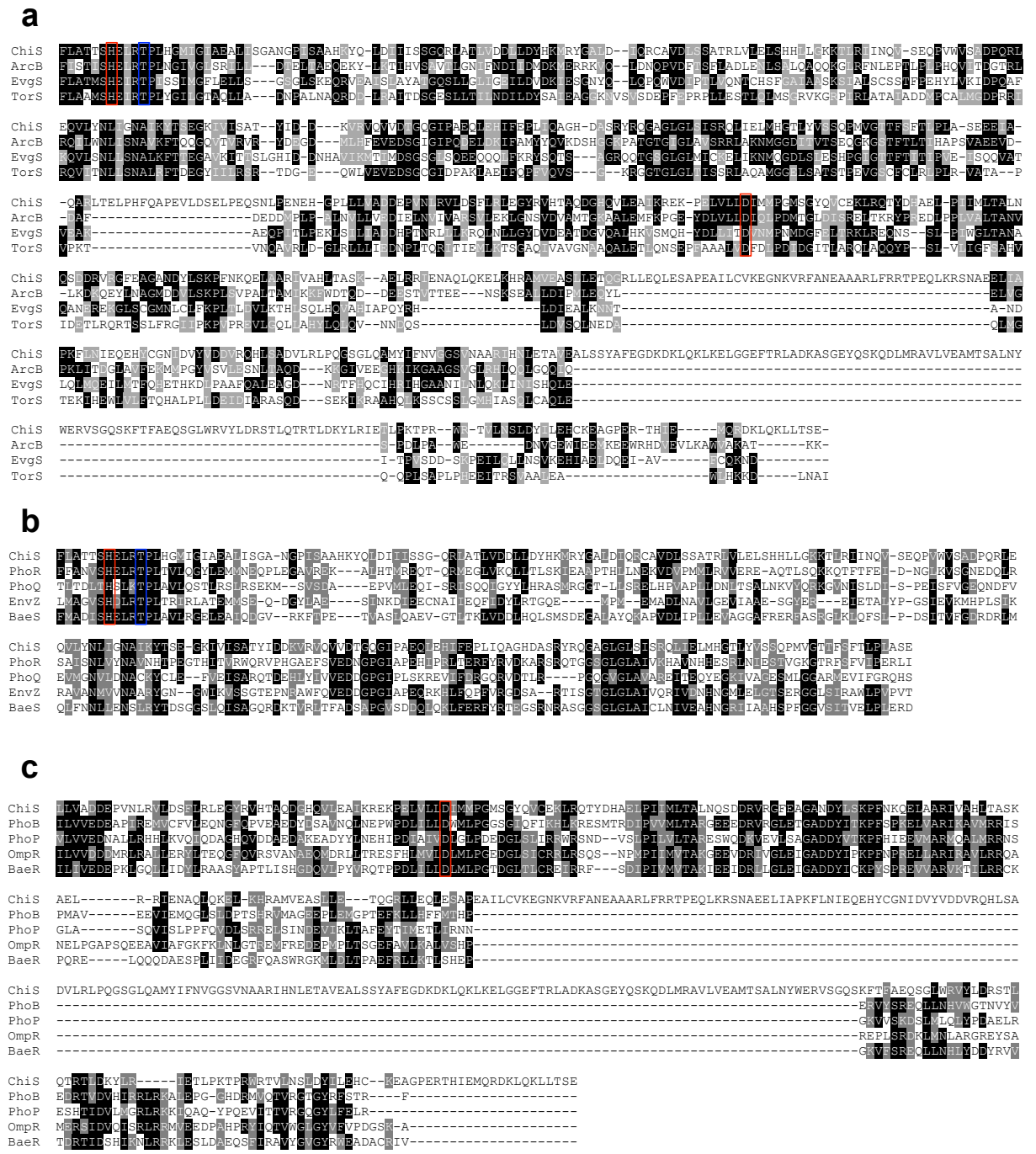

Fig. S1. *ChiS is a hybrid histidine kinase.* Alignment of ChiS with (**a**) other hybrid sensor kinases (ArcB, EvgS, and TorS) starting at the H box (47), (**b**) histidine kinases (PhoR, PhoQ, EnvZ, and BaeS) starting at the H box (47), and (**c**) response regulators (PhoB, PhoP, OmpR, and BaeR) starting at the receiver domain. All protein sequences for alignment with *V. cholerae* ChiS are from *E. coli* MG1655. The conserved sites of phosphorylation (red boxes) and the threonine critical for phosphatase activity (blue box) are highlighted. Residues highlighted in black are identical, while those highlighted in gray are similar.

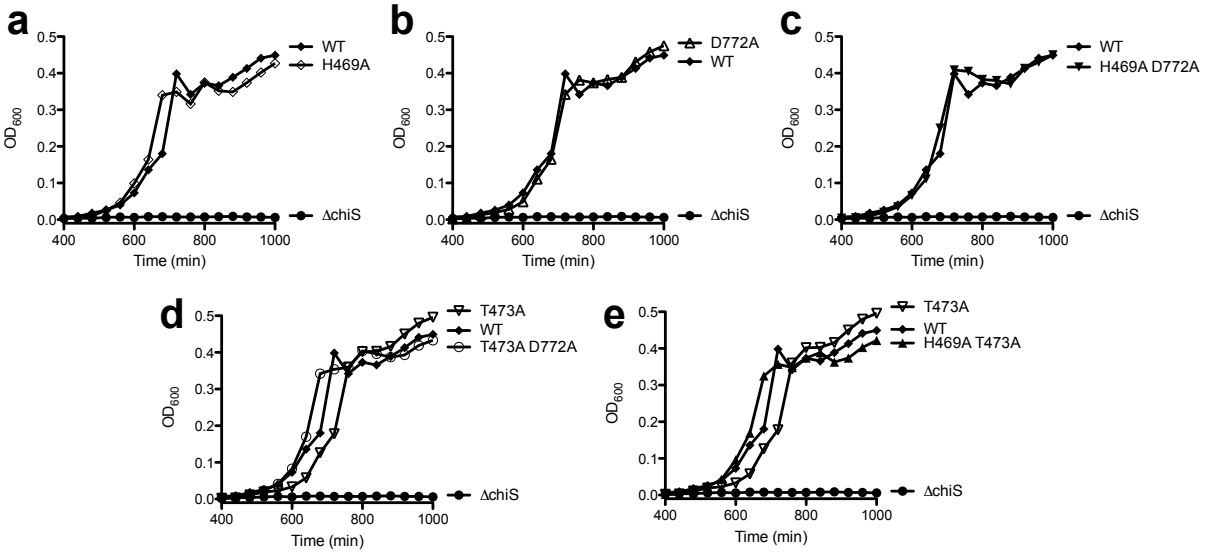

Fig. S2. *Strains that activate P_{chb} grow like WT on chitobiose*. Strains harboring the indicated point mutations in ChiS were tested for growth on M9 minimal medium containing chitobiose as the sole carbon source. Data for WT, Δ*chiS*, and T473A are identical to the data presented in **Fig. 1b**, and included in relevant panels for ease of comparison. Data are representative of two independent experiments.

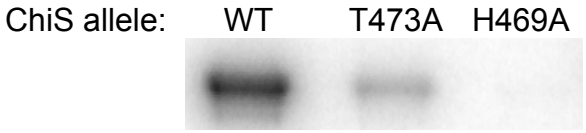

Fig. S3. *ChiS exhibits kinase activity in vitro*. Purified ChiS (MBP-ChiS^{cytoplasmic}) containing the indicated mutations were assessed for autokinase activity *in vitro* using ^{32}P-labelled ATP. Data are representative of two independent experiments.

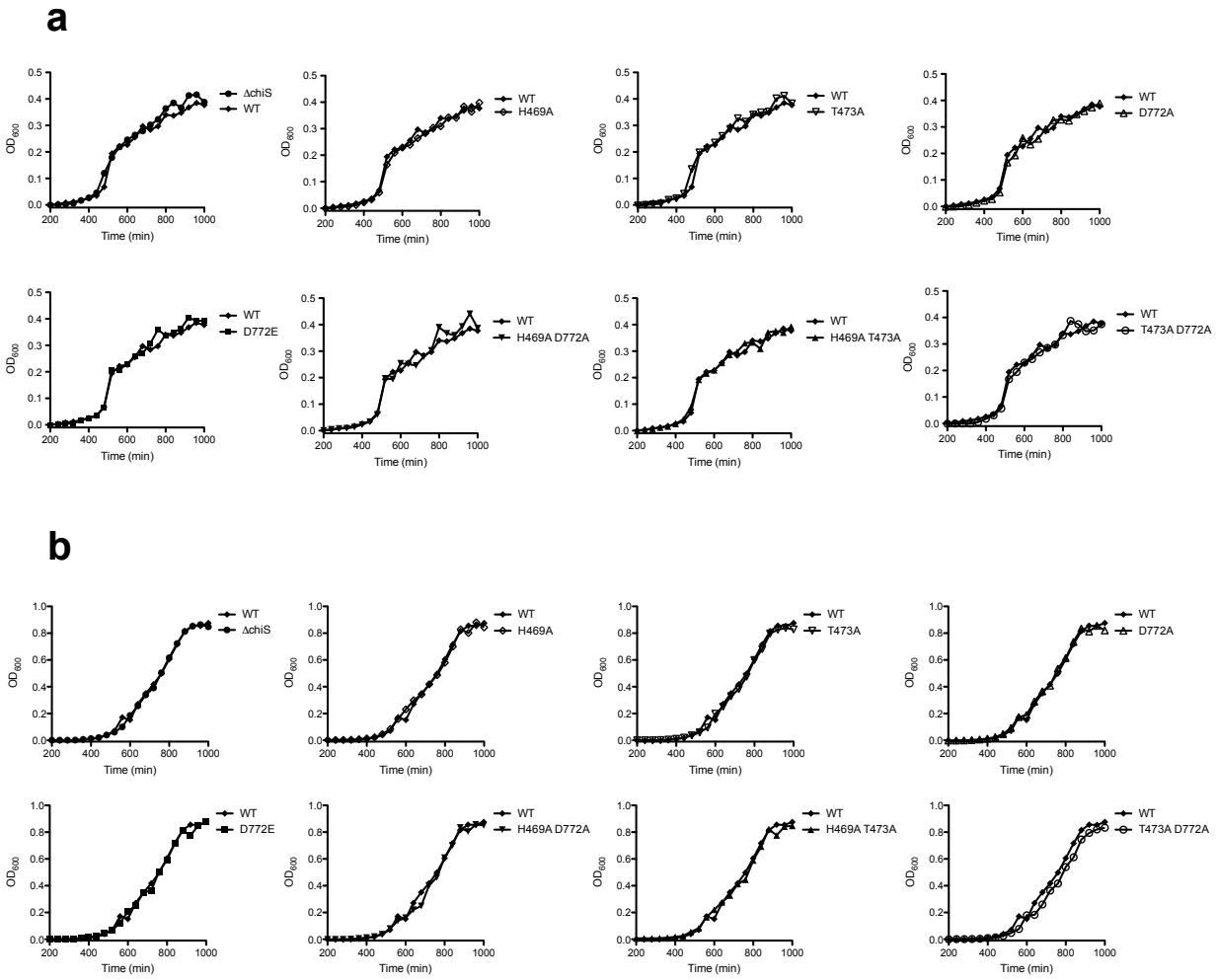

Fig. S4. *Mutations in ChiS do not alter growth on other carbon sources*. Strains harboring the indicated mutations in ChiS were tested for growth on minimal medium containing tryptone (**a**) or glucose (**b**) as the sole carbon source. WT curves for each carbon source are identical in each panel and included for ease of comparison. Data are representative of two independent experiments.

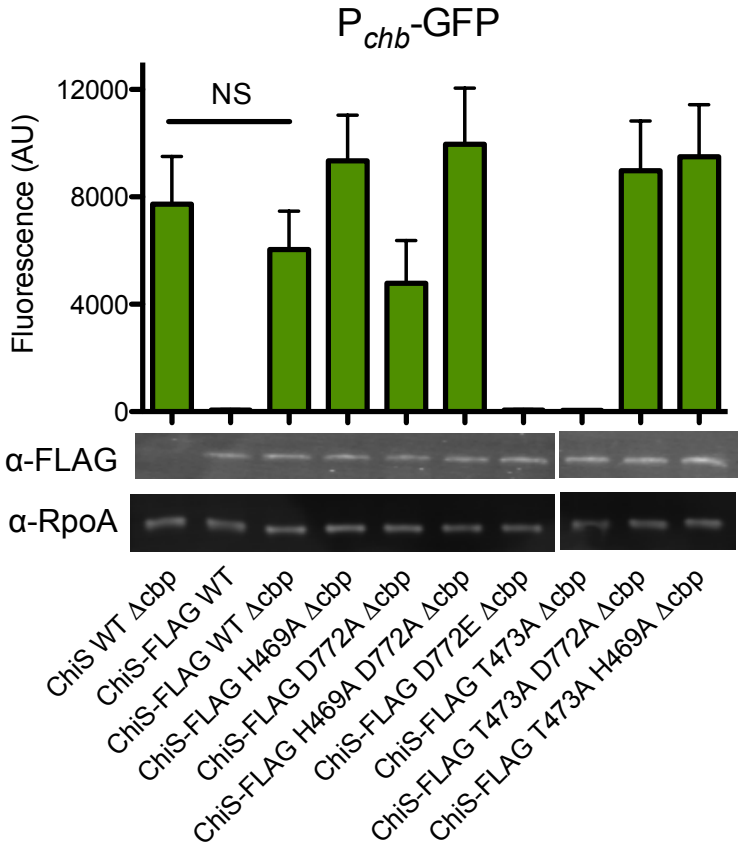

Fig. S5. *ChiS-FLAG is functional and ChiS expression does not change when residues critical for phosphorylation or phosphatase activity are mutated*. FLAG-tagged ChiS alleles were assessed for functionality using a P_{chb}-GFP reporter and expression of ChiS was assessed by Western blot analysis. P_{chb}-GFP results confirm that ChiS-FLAG functions similar to untagged ChiS (as shown in **Fig. 1**). Western blot results demonstrate that mutating residues critical for phosphorylation (H469, D772) or phosphatase activity (T473) do not alter ChiS protein levels. P_{chb}-GFP data are the result of at least three independent biological replicates and shown as the mean ± SD. Western blot results are representative of two independent experiments. Statistical comparisons were made by one-way ANOVA with Tukey's post-test. NS, not significant.

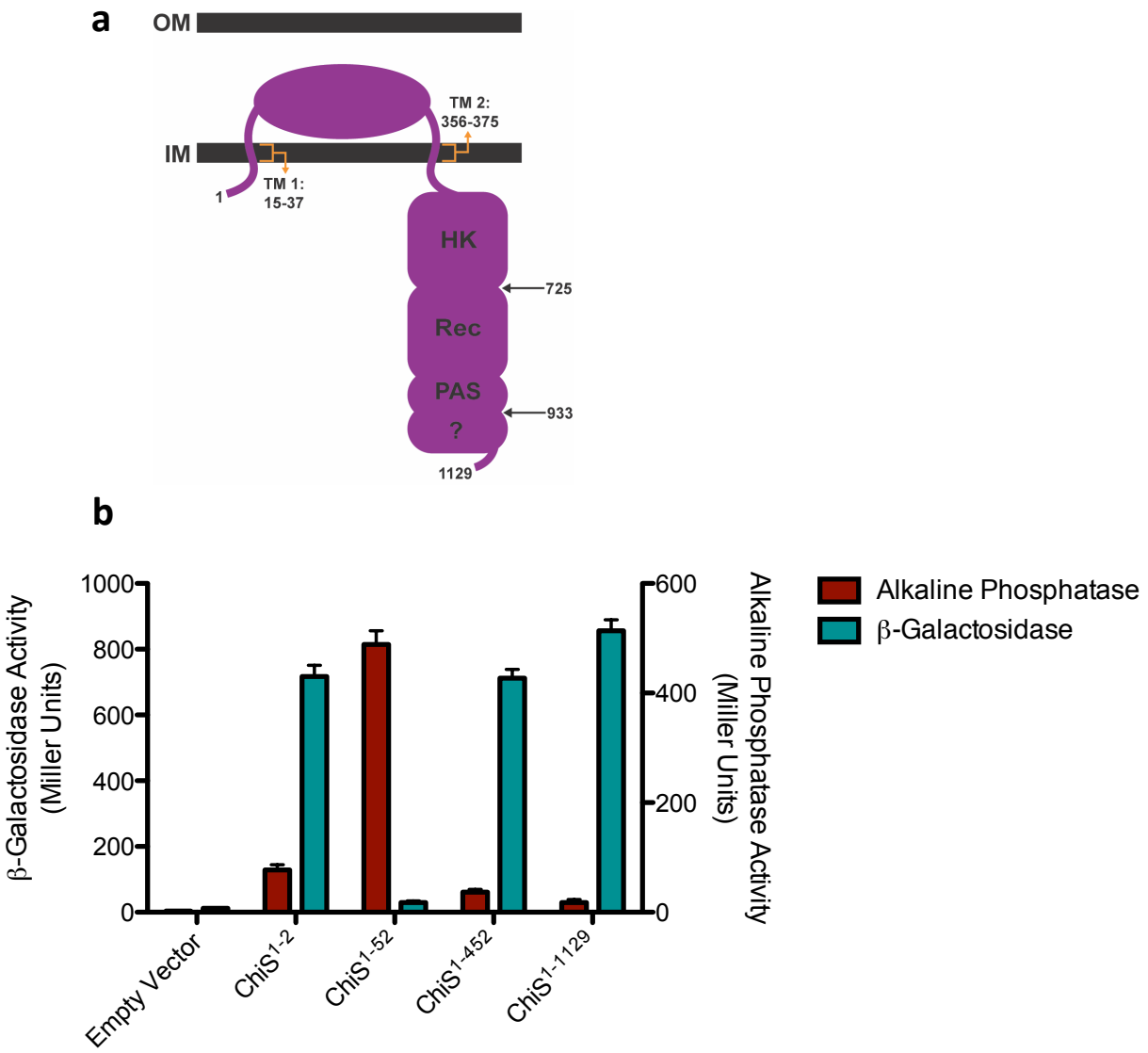

Fig. S6. *Testing ChiS membrane topology*. (**a**) ChiS predicted membrane topology with transmembrane (TM), histidine kinase (HK), receiver (Rec), and Per-Arnt-Sim (PAS) domains labeled with residue numbers. (**b**) The indicated ChiS C-terminal truncations were fused to *lacZ* or *phoA* and then assessed for beta-galactosidase and alkaline phosphatase activity, respectively. All data are the result of at least three independent biological replicates and shown as the mean ± SD.

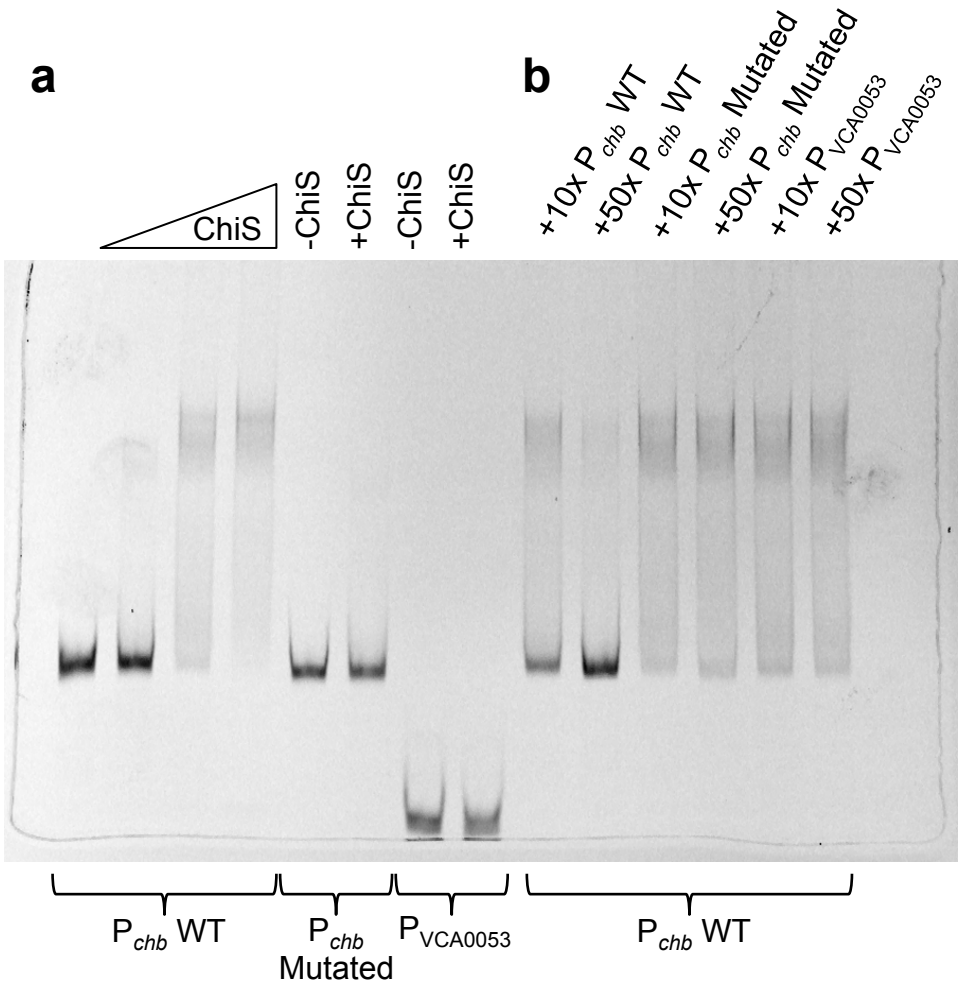

Fig. S7. *ChiS binds to the P_{chb} promoter.* (**a**) EMSA assays were carried out using a purified portion of the ChiS cytoplasmic domain ($ChiS^{Rec\text{-}C}$) and the Cy5-labeled DNA probe indicated below the gel. For lanes 1-4, a fixed concentration of the minimal fragment of the P_{chb} promoter required for activation(7) (P_{chb} WT) was incubated with increasing concentrations of ChiS (from left to right: 0 nM, 50 nM, 100 nM, 200 nM). A probe where the two ChiS binding sites within P_{chb} were mutated (P_{chb} Mutated – see **Fig. 3c** for details) and a negative control probe that represents a promoter not regulated by ChiS ($P_{VCA0053}$) were incubated with no ChiS (-ChiS) or 200 nM ChiS (+ChiS). (**b**) Cold competitor EMSAs were carried out using reactions where 100 nM ChiS was incubated with a fixed concentration of Cy5 labeled P_{chb} WT probe and either a 10x or 50x fold-excess of the unlabeled competitor DNA indicated above the gel. These data indicate that ChiS binding to P_{chb} WT can only be competed off by specific DNA (unlabeled P_{chb} WT) but not nonspecific DNA ($P_{VCA0053}$) or the probe where both ChiS binding sites in P_{chb} are mutated (P_{chb} Mutated). Data are representative of two independent experiments.

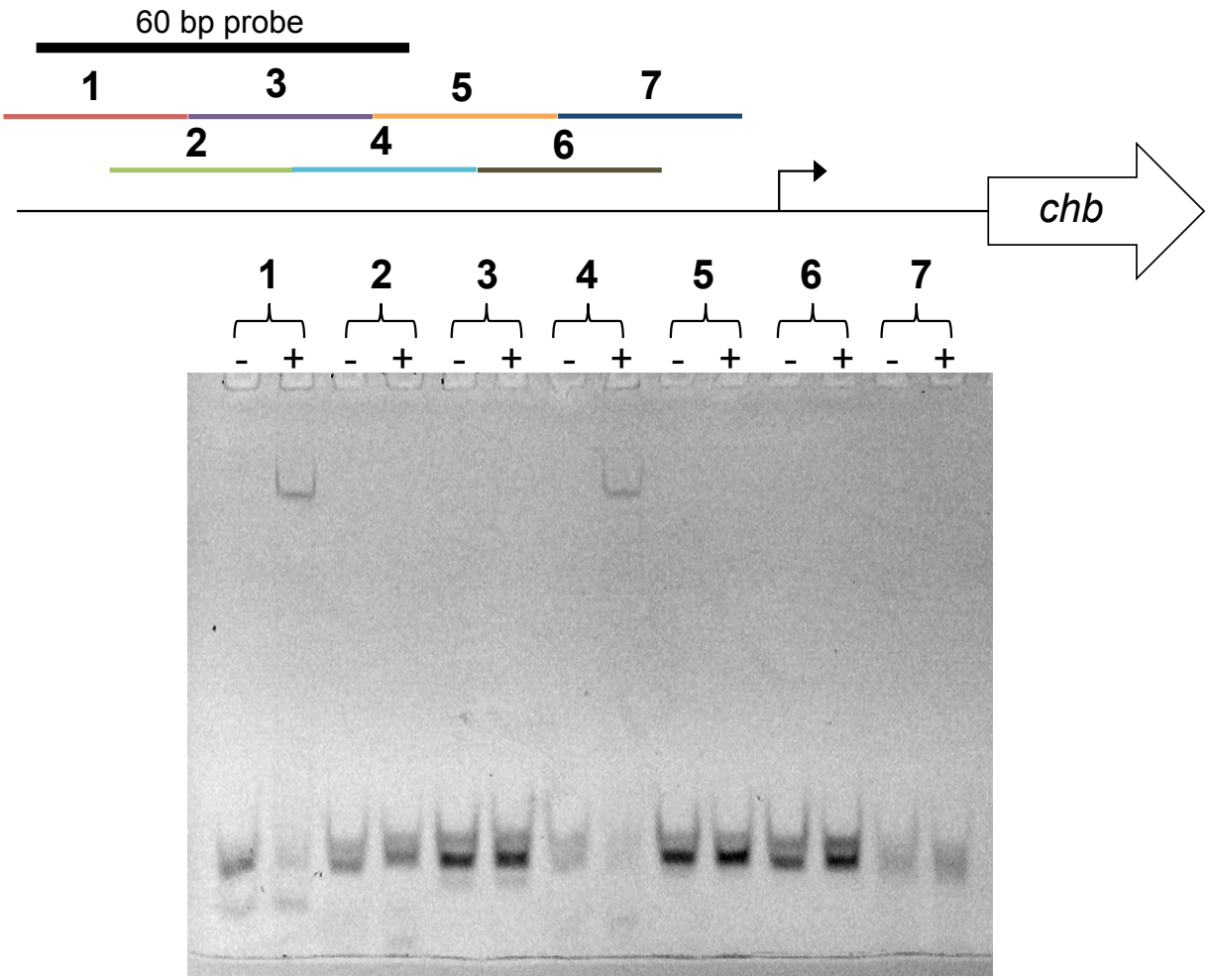

Fig. S8. *ChiS binds two sites within the P_{chb} promoter*. EMSA reactions were carried out using a purified portion of the ChiS cytoplasmic domain ($ChiS^{Rec\text{-}C}$) and Cy5 labeled 30 bp overlapping segments of P_{chb} (labeled 1-7). Probes were incubated with no ChiS (-) or 200 nM ChiS (+). The 60 bp probe containing both ChiS binding sites used in **Fig. 3a** is also indicated on the schematic. Data are representative of two independent experiments.

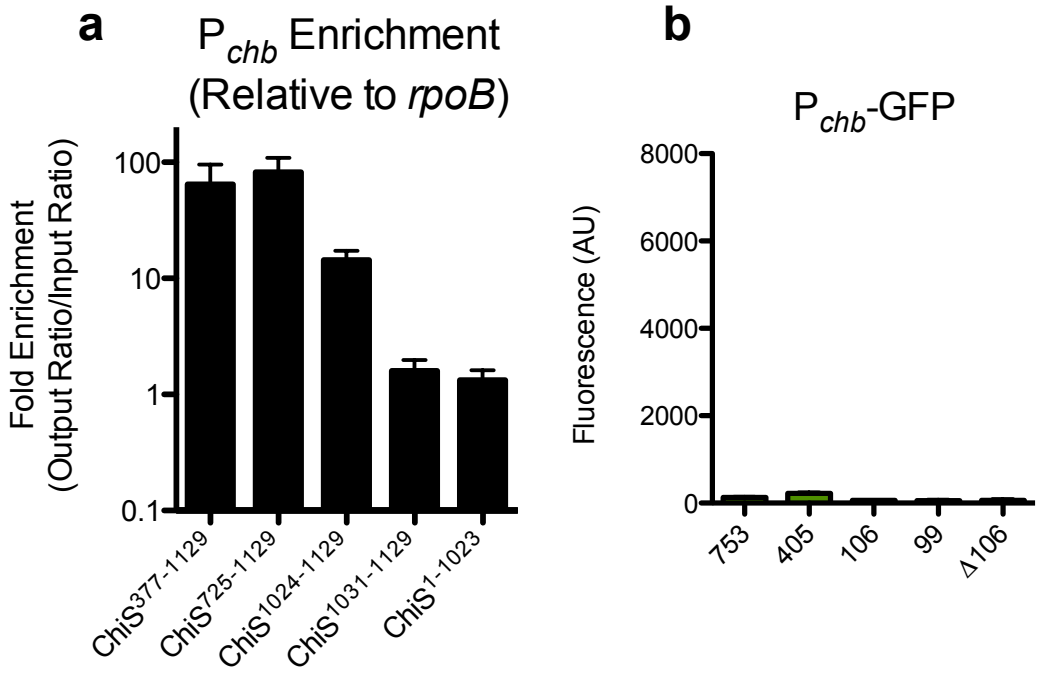

Fig. S9. *The last 106 amino acids of ChiS is necessary and sufficient to bind P_{chb}, but does not activate P_{chb}.* (**a**) ChIP assays were carried out in *V. cholerae* strains overexpressing N-terminal truncations of ChiS (first 4 bars) or natively expressing ChiS with a C-terminal truncation of the last 106 amino acids (last bar). (**b**) The same strains indicated in **a** were assessed for activation of a P_{chb}-GFP reporter. All data are from at least three independent biological replicates and shown as the mean ± SD.

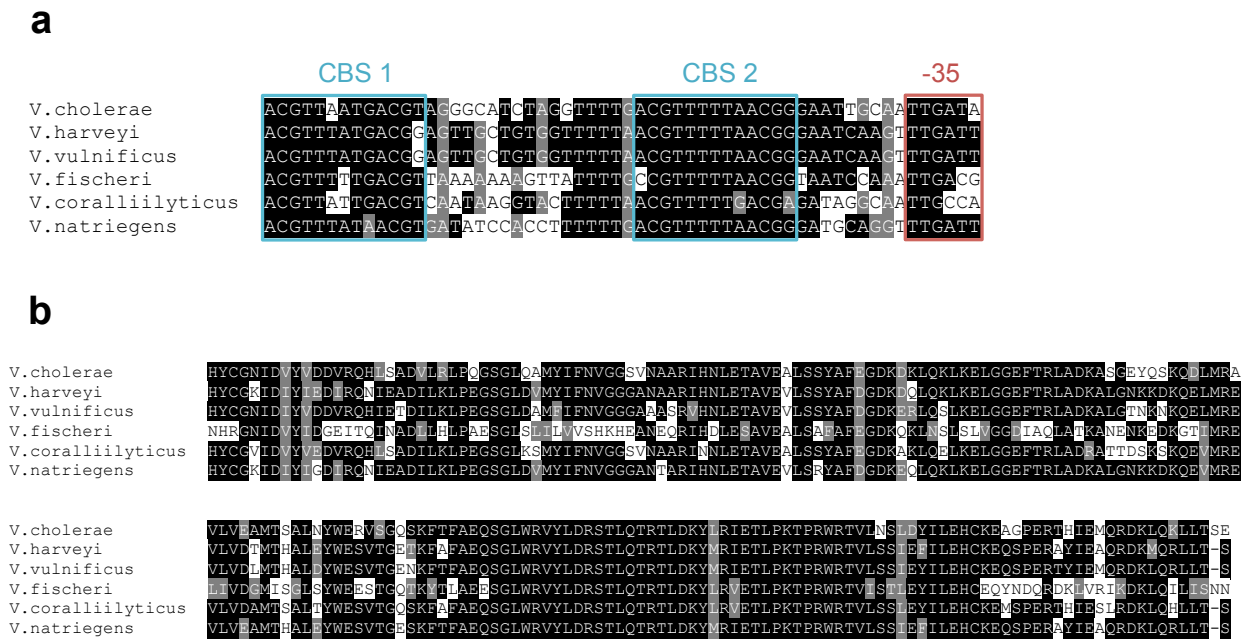

Fig. S10. *The ChiS binding sites (CBSs) in P_{chb} and the ChiS C-terminus are conserved among Vibrio* species. (**a**) A section of the P_{chb} DNA sequence (CBS 1 until the -35 signal) from the indicated *Vibrio* species were aligned. CBSs are boxed in blue and the -35 signal is boxed in red. (**b**) The last 197 amino acids of *V. cholerae* ChiS, which contains a cryptic DNA binding domain, was aligned to the C-terminal domains of ChiS homologs from the indicated *Vibrio* species. Residues highlighted in black are identical, those highlighted in gray are similar.

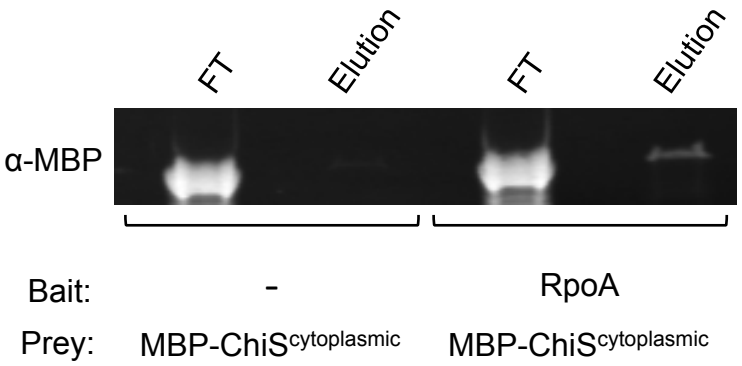

Fig. S11. *ChiS and RpoA interact in vitro.* A protein pulldown using purified RpoA as bait and purified ChiS (MBP-ChiS^{cytoplasmic}) as prey was carried out. The presence of the MBP-ChiS^{cytoplasmic} prey was assessed in the flow through (FT) and elution by Western blot analysis. Data are representative of two independent experiments.

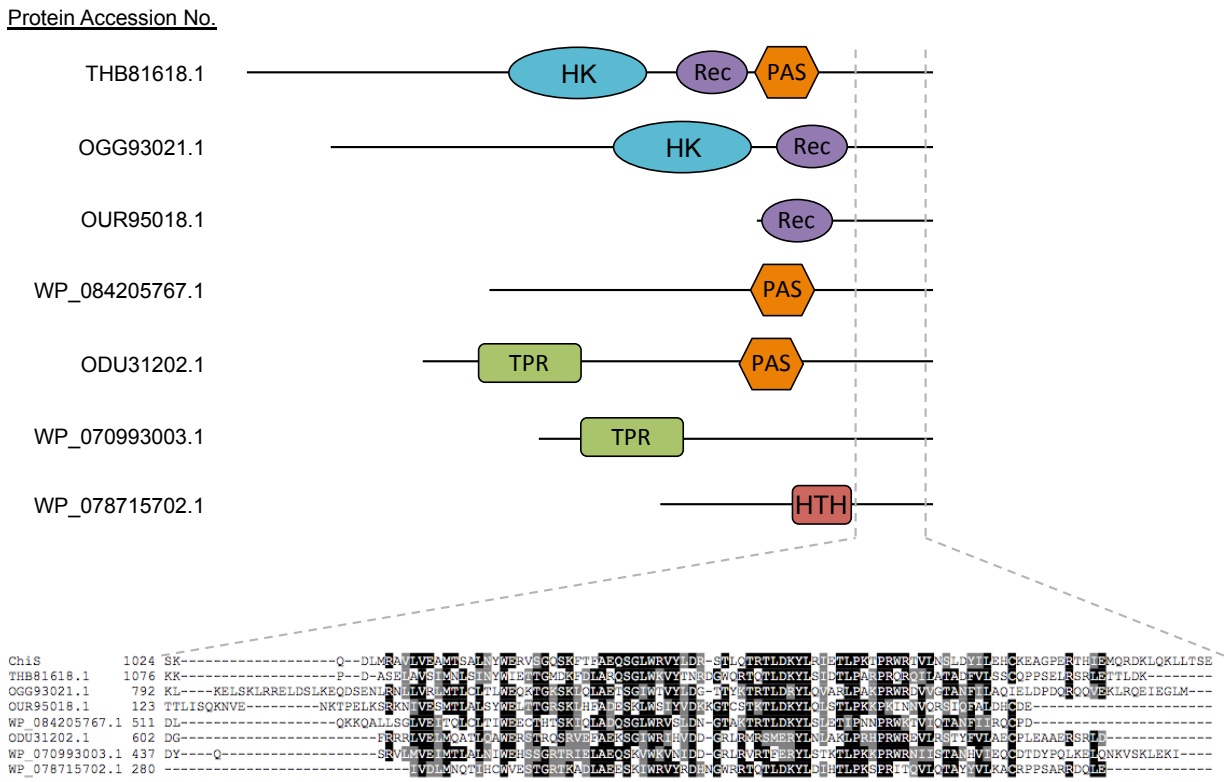

Fig. S12. *Representative examples of BLAST hits containing putative ChiS-like C-terminal DNA binding domains*. Various hits from BLAST hits gave proteins that contain histidine kinase (HK), receiver (Rec), Per-ARNT-Sim (PAS), tetratricopeptide protein repeat (TPR), and helix-turn-helix (HTH) domains. The C-terminal domains of the indicated proteins were aligned against the last 106 amino acids of ChiS. Residues highlighted in black are identical, while those highlighted in gray are similar.

Table S1 – *Full list of statistical comparisons made in this manuscript*

Comparison	p-Value	
Figure 1A – Tukey's Multiple Comparison's Test		
WT vs. WT Δcbp	****	<0.0001
WT vs. ΔchiS Δcbp	ns	>0.9999
WT vs. H469A	****	<0.0001
WT vs. H469A Δcbp	****	<0.0001
WT vs. T473A	ns	>0.9999
WT vs. T473A Δcbp	ns	>0.9999
WT vs. D772A	ns	0.9916
WT vs. D772A Δcbp	****	<0.0001
WT vs. D772E	ns	>0.9999
WT vs. D772E Δcbp	ns	>0.9999
WT vs. T473A H469A Δcbp	****	<0.0001
WT vs. T473A H469A Δcbp	****	<0.0001
WT vs. H469A D772A	****	<0.0001
WT vs. H469A D772A Δcbp	****	<0.0001
WT vs. T473A D772A	**	0.0084
WT vs. T473A D772A Δcbp	****	<0.0001
WT Δcbp vs. ΔchiS Δcbp	****	<0.0001
WT Δcbp vs. H469A	****	<0.0001
WT Δcbp vs. H469A Δcbp	****	<0.0001
WT Δcbp vs. T473A	****	<0.0001
WT Δcbp vs. T473A Δcbp	****	<0.0001
WT Δcbp vs. D772A	****	<0.0001
WT Δcbp vs. D772A Δcbp	****	<0.0001
WT Δcbp vs. D772E	****	<0.0001
WT Δcbp vs. D772E Δcbp	****	<0.0001
WT Δcbp vs. T473A H469A Δcbp	****	<0.0001
WT Δcbp vs. T473A H469A Δcbp	****	<0.0001
WT Δcbp vs. H469A D772A	****	<0.0001
WT Δcbp vs. H469A D772A Δcbp	****	<0.0001
WT Δcbp vs. T473A D772A	****	<0.0001
WT Δcbp vs. T473A D772A Δcbp	****	<0.0001
ΔchiS Δcbp vs. H469A	****	<0.0001
ΔchiS Δcbp vs. H469A Δcbp	****	<0.0001
ΔchiS Δcbp vs. T473A	ns	>0.9999
ΔchiS Δcbp vs. T473A Δcbp	ns	>0.9999
ΔchiS Δcbp vs. D772A	ns	0.9974
ΔchiS Δcbp vs. D772A Δcbp	****	<0.0001
ΔchiS Δcbp vs. D772E	ns	>0.9999
ΔchiS Δcbp vs. D772E Δcbp	ns	>0.9999

ΔchiS Δcbp vs. T473A H469A Δcbp	****	<0.0001
ΔchiS Δcbp vs. T473A H469A Δcbp	****	<0.0001
ΔchiS Δcbp vs. H469A D772A	****	<0.0001
ΔchiS Δcbp vs. H469A D772A Δcbp	****	<0.0001
ΔchiS Δcbp vs. T473A D772A	*	0.0425
ΔchiS Δcbp vs. T473A D772A Δcbp	****	<0.0001
H469A vs. H469A Δcbp	****	<0.0001
H469A vs. T473A	****	<0.0001
H469A vs. T473A Δcbp	****	<0.0001
H469A vs. D772A	****	<0.0001
H469A vs. D772A Δcbp	****	<0.0001
H469A vs. D772E	****	<0.0001
H469A vs. D772E Δcbp	****	<0.0001
H469A vs. T473A H469A Δcbp	ns	0.0815
H469A vs. T473A H469A Δcbp	****	<0.0001
H469A vs. H469A D772A	ns	0.9587
H469A vs. H469A D772A Δcbp	****	<0.0001
H469A vs. T473A D772A	*	0.0491
H469A vs. T473A D772A Δcbp	****	<0.0001
H469A Δcbp vs. T473A	****	<0.0001
H469A Δcbp vs. T473A Δcbp	****	<0.0001
H469A Δcbp vs. D772A	****	<0.0001
H469A Δcbp vs. D772A Δcbp	****	<0.0001
H469A Δcbp vs. D772E	****	<0.0001
H469A Δcbp vs. D772E Δcbp	****	<0.0001
H469A Δcbp vs. T473A H469A Δcbp	****	<0.0001
H469A Δcbp vs. T473A H469A Δcbp	ns	0.1749
H469A Δcbp vs. H469A D772A	****	<0.0001
H469A Δcbp vs. H469A D772A Δcbp	*	0.0163
H469A Δcbp vs. T473A D772A	****	<0.0001
H469A Δcbp vs. T473A D772A Δcbp	**	0.0034
T473A vs. T473A Δcbp	ns	>0.9999
T473A vs. D772A	ns	0.9977
T473A vs. D772A Δcbp	****	<0.0001
T473A vs. D772E	ns	>0.9999
T473A vs. D772E Δcbp	ns	>0.9999
T473A vs. T473A H469A Δcbp	****	<0.0001
T473A vs. T473A H469A Δcbp	****	<0.0001
T473A vs. H469A D772A	****	<0.0001
T473A vs. H469A D772A Δcbp	****	<0.0001
T473A vs. T473A D772A	*	0.0441
T473A vs. T473A D772A Δcbp	****	<0.0001
T473A Δcbp vs. D772A	ns	>0.9999

T473A Δcbp vs. D772A Δcbp	****	<0.0001
T473A Δcbp vs. D772E	ns	>0.9999
T473A Δcbp vs. D772E Δcbp	ns	>0.9999
T473A Δcbp vs. T473A H469A Δcbp	****	<0.0001
T473A Δcbp vs. T473A H469A Δcbp	****	<0.0001
T473A Δcbp vs. H469A D772A	**	0.0014
T473A Δcbp vs. H469A D772A Δcbp	****	<0.0001
T473A Δcbp vs. T473A D772A	ns	0.3546
T473A Δcbp vs. T473A D772A Δcbp	****	<0.0001
D772A vs. D772A Δcbp	****	<0.0001
D772A vs. D772E	ns	0.9977
D772A vs. D772E Δcbp	ns	0.9995
D772A vs. T473A H469A Δcbp	****	<0.0001
D772A vs. T473A H469A Δcbp	****	<0.0001
D772A vs. H469A D772A	**	0.0058
D772A vs. H469A D772A Δcbp	****	<0.0001
D772A vs. T473A D772A	ns	0.6259
D772A vs. T473A D772A Δcbp	****	<0.0001
D772A Δcbp vs. D772E	****	<0.0001
D772A Δcbp vs. D772E Δcbp	****	<0.0001
D772A Δcbp vs. T473A H469A Δcbp	****	<0.0001
D772A Δcbp vs. T473A H469A Δcbp	****	<0.0001
D772A Δcbp vs. H469A D772A	****	<0.0001
D772A Δcbp vs. H469A D772A Δcbp	****	<0.0001
D772A Δcbp vs. T473A D772A	****	<0.0001
D772A Δcbp vs. T473A D772A Δcbp	****	<0.0001
D772E vs. D772E Δcbp	ns	>0.9999
D772E vs. T473A H469A Δcbp	****	<0.0001
D772E vs. T473A H469A Δcbp	****	<0.0001
D772E vs. H469A D772A	****	<0.0001
D772E vs. H469A D772A Δcbp	****	<0.0001
D772E vs. T473A D772A	*	0.0444
D772E vs. T473A D772A Δcbp	****	<0.0001
D772E Δcbp vs. T473A H469A Δcbp	****	<0.0001
D772E Δcbp vs. T473A H469A Δcbp	****	<0.0001
D772E Δcbp vs. H469A D772A	****	<0.0001
D772E Δcbp vs. H469A D772A Δcbp	****	<0.0001
D772E Δcbp vs. T473A D772A	ns	0.069
D772E Δcbp vs. T473A D772A Δcbp	****	<0.0001
T473A H469A Δcbp vs. T473A H469A Δcbp	****	<0.0001
T473A H469A Δcbp vs. H469A D772A	***	0.0003
T473A H469A Δcbp vs. H469A D772A Δcbp	****	<0.0001

T473A H469A Δcbp vs. T473A D772A	****	<0.0001
T473A H469A Δcbp vs. T473A D772A Δcbp	****	<0.0001
T473A H469A Δcbp vs. H469A D772A	****	<0.0001
T473A H469A Δcbp vs. H469A D772A Δcbp	ns	>0.9999
T473A H469A Δcbp vs. T473A D772A	****	<0.0001
T473A H469A Δcbp vs. T473A D772A Δcbp	ns	0.9965
H469A D772A vs. H469A D772A Δcbp	****	<0.0001
H469A D772A vs. T473A D772A	ns	0.895
H469A D772A vs. T473A D772A Δcbp	****	<0.0001
H469A D772A Δcbp vs. T473A D772A	****	<0.0001
H469A D772A Δcbp vs. T473A D772A Δcbp	ns	>0.9999
T473A D772A vs. T473A D772A Δcbp	****	<0.0001
Figure 2A-Miller Assay – Tukey's Multiple Comparison's Test		
Empty Vector vs. ChiS WT	****	<0.0001
Empty Vector vs. ChiS D772E	*	0.0385
ChiS WT vs. ChiS D772E	****	<0.0001
Figure 2A-ChIP – Student's t-Test		
ChiS WT vs. ChiS D772E	ns	0.1187
Figure 2B-GFP Assay – Tukey's Multiple Comparison's Test		
ChiS FLAG cyto cbp+ vs. ChiS FLAG cyto Δcbp	****	<0.0001
ChiS FLAG cyto cbp+ vs. ChiS FLAG cyto D772E Δcbp	ns	>0.9999
ChiS FLAG cyto cbp+ vs. Ptac-ChiS FLAG cyto Δcbp	****	<0.0001
ChiS FLAG cyto cbp+ vs. Ptac-ChiS FLAG cyto D772E Δcbp	***	0.0001
ChiS FLAG cyto cbp+ vs. ChiS FLAG peri Δcbp	****	<0.0001
ChiS FLAG cyto Δcbp vs. ChiS FLAG cyto D772E Δcbp	****	<0.0001
ChiS FLAG cyto Δcbp vs. Ptac-ChiS FLAG cyto Δcbp	****	<0.0001
ChiS FLAG cyto Δcbp vs. Ptac-ChiS FLAG cyto D772E Δcbp	****	<0.0001
ChiS FLAG cyto Δcbp vs. ChiS FLAG peri Δcbp	ns	0.404
ChiS FLAG cyto D772E Δcbp vs. Ptac-ChiS FLAG cyto Δcbp	****	<0.0001
ChiS FLAG cyto D772E Δcbp vs. Ptac-ChiS FLAG cyto D772E Δcbp	***	0.0002
ChiS FLAG cyto D772E Δcbp vs. ChiS FLAG peri Δcbp	****	<0.0001
Ptac-ChiS FLAG cyto Δcbp vs. Ptac-ChiS FLAG cyto D772E Δcbp	****	<0.0001
Ptac-ChiS FLAG cyto Δcbp vs. ChiS FLAG peri Δcbp	****	<0.0001
Ptac-ChiS FLAG cyto D772E Δcbp vs. ChiS FLAG peri Δcbp	****	<0.0001
Figure 2B-ChIP – Tukey's Multiple Comparison's Test		
ChiS-FLAG cyto WT cbp+ vs. ChiS-FLAG cyto WT Δcbp	**	0.0039
ChiS-FLAG cyto WT cbp+ vs. ChiS-FLAG cyto D772E Δcbp	ns	>0.9999
ChiS-FLAG cyto WT cbp+ vs. Ptac-ChiS-FLAG cyto WT Δcbp	**	0.0023
ChiS-FLAG cyto WT cbp+ vs. Ptac-ChiS-FLAG cyto D772E Δcbp	**	0.0018
ChiS-FLAG cyto WT cbp+ vs. ChiS FLAG peri Δcbp	**	0.0012
ChiS-FLAG cyto WT Δcbp vs. ChiS-FLAG cyto D772E Δcbp	**	0.0032
ChiS-FLAG cyto WT Δcbp vs. Ptac-ChiS-FLAG cyto WT Δcbp	ns	0.9827

ChiS-FLAG cyto WT Δcbp vs. Ptac-ChiS-FLAG cyto D772E Δcbp	ns	0.9605
ChiS-FLAG cyto WT Δcbp vs. ChiS FLAG peri Δcbp	ns	0.8879
ChiS-FLAG cyto D772E Δcbp vs. Ptac-ChiS-FLAG cyto WT Δcbp	**	0.0019
ChiS-FLAG cyto D772E Δcbp vs. Ptac-ChiS-FLAG cyto D772E Δcbp	**	0.0015
ChiS-FLAG cyto D772E Δcbp vs. ChiS FLAG peri Δcbp	**	0.001
Ptac-ChiS-FLAG cyto WT Δcbp vs. Ptac-ChiS-FLAG cyto D772E Δcbp	ns	>0.9999
Ptac-ChiS-FLAG cyto WT Δcbp vs. ChiS FLAG peri Δcbp	ns	0.9989
Ptac-ChiS-FLAG cyto D772E Δcbp vs. ChiS FLAG peri Δcbp	ns	0.9999
Figure 3C – Tukey's Multiple Comparison's Test		
WT vs. WT Δcbp	****	<0.0001
WT vs. BS 1 Mutate	ns	>0.9999
WT vs. BS 1 Mutate Δcbp	***	0.0002
WT vs. BS 2 Mutate	ns	>0.9999
WT vs. BS 2 Mutate Δcbp	*	0.0231
WT vs. BS 1 & 2 Mutate	ns	>0.9999
WT vs. BS 1 & 2 Mutate Δcbp	ns	>0.9999
WT Δcbp vs. BS 1 Mutate	****	<0.0001
WT Δcbp vs. BS 1 Mutate Δcbp	****	<0.0001
WT Δcbp vs. BS 2 Mutate	****	<0.0001
WT Δcbp vs. BS 2 Mutate Δcbp	****	<0.0001
WT Δcbp vs. BS 1 & 2 Mutate	****	<0.0001
WT Δcbp vs. BS 1 & 2 Mutate Δcbp	****	<0.0001
BS 1 Mutate vs. BS 1 Mutate Δcbp	***	0.0004
BS 1 Mutate vs. BS 2 Mutate	ns	>0.9999
BS 1 Mutate vs. BS 2 Mutate Δcbp	*	0.0488
BS 1 Mutate vs. BS 1 & 2 Mutate	ns	>0.9999
BS 1 Mutate vs. BS 1 & 2 Mutate Δcbp	ns	>0.9999
BS 1 Mutate Δcbp vs. BS 2 Mutate	***	0.0002
BS 1 Mutate Δcbp vs. BS 2 Mutate Δcbp	ns	0.7113
BS 1 Mutate Δcbp vs. BS 1 & 2 Mutate	***	0.0006
BS 1 Mutate Δcbp vs. BS 1 & 2 Mutate Δcbp	***	0.0003
BS 2 Mutate vs. BS 2 Mutate Δcbp	*	0.0252
BS 2 Mutate vs. BS 1 & 2 Mutate	ns	>0.9999
BS 2 Mutate vs. BS 1 & 2 Mutate Δcbp	ns	>0.9999
BS 2 Mutate Δcbp vs. BS 1 & 2 Mutate	ns	0.0584
BS 2 Mutate Δcbp vs. BS 1 & 2 Mutate Δcbp	*	0.0382
BS 1 & 2 Mutate vs. BS 1 & 2 Mutate Δcbp	ns	>0.9999
Figure 4B – Tukey's Multiple Comparison's Test		
A: 0 B: 0 vs. A: +5	****	<0.0001
A: 0 B: 0 vs. A: +10	****	<0.0001
A: 0 B: 0 vs. B: +5	****	<0.0001
A: 0 B: 0 vs. B: +10	****	<0.0001

A: 0 B: 0 vs. B: -5	****	<0.0001
A: 0 B: 0 vs. B: -10	****	<0.0001
A: 0 B: 0 vs. A: +5 B: +5	****	<0.0001
A: 0 B: 0 vs. A: +5 B: -5	****	<0.0001
A: +5 vs. A: +10	****	<0.0001
A: +5 vs. B: +5	ns	>0.9999
A: +5 vs. B: +10	****	<0.0001
A: +5 vs. B: -5	ns	>0.9999
A: +5 vs. B: -10	****	<0.0001
A: +5 vs. A: +5 B: +5	ns	>0.9999
A: +5 vs. A: +5 B: -5	ns	>0.9999
A: +10 vs. B: +5	****	<0.0001
A: +10 vs. B: +10	***	0.0004
A: +10 vs. B: -5	****	<0.0001
A: +10 vs. B: -10	**	0.0073
A: +10 vs. A: +5 B: +5	****	<0.0001
A: +10 vs. A: +5 B: -5	****	<0.0001
B: +5 vs. B: +10	****	<0.0001
B: +5 vs. B: -5	ns	>0.9999
B: +5 vs. B: -10	****	<0.0001
B: +5 vs. A: +5 B: +5	ns	>0.9999
B: +5 vs. A: +5 B: -5	ns	>0.9999
B: +10 vs. B: -5	****	<0.0001
B: +10 vs. B: -10	ns	0.9972
B: +10 vs. A: +5 B: +5	****	<0.0001
B: +10 vs. A: +5 B: -5	****	<0.0001
B: -5 vs. B: -10	****	<0.0001
B: -5 vs. A: +5 B: +5	ns	>0.9999
B: -5 vs. A: +5 B: -5	ns	>0.9999
B: -10 vs. A: +5 B: +5	****	<0.0001
B: -10 vs. A: +5 B: -5	****	<0.0001
A: +5 B: +5 vs. A: +5 B: -5	ns	>0.9999

Table S2 – *Strains used in this manuscript*

Reference (Strain Designation)	Reference in Manuscript	Genotype
(33) (SAD 030)	Parent strain for all other *V. cholerae* strains in this study	*V. cholerae* WT E7946 Sm^R
This study (CAK 967/ SAD 2670)	Fig. 1A D772E cbp+	P_{chb}-GFP @ lacZ, KanR; ΔchiS::CarbR; P_{chiS}-ChiS D772E @ VCA0692, TmR
This study (CAK 968/ SAD 2671)	Fig. 1A D772E Δcbp	P_{chb}-GFP @ lacZ, KanR; ΔchiS/cbp::CarbR; P_{chiS}-ChiS D772E @ VCA0692, TmR
This study (CAK 999/ SAD 2672)	Fig. 1A T473A cbp+	P_{chb}-GFP @ lacZ, KanR; P_{chiS}-ChiS T473A @ VCA0692, TmR; ΔchiS::CarbR
This study (CAK 1000/ SAD 2673)	Fig. 1A T473A Δcbp	P_{chb}-GFP @ lacZ, KanR; P_{chiS}-ChiS T473A @ VCA0692, TmR; ΔchiS/cbp::CarbR
This study (CAK 1017/ SAD 2674)	Fig. 1A T473A D772A Δcbp	P_{chb}-GFP @ lacZ, KanR; P_{chiS}-ChiS T473A D772A @ VCA0692, TmR; ΔchiS/cbp::CarbR
This study (CAK 1030/ SAD 2675)	Fig. 1A & S5 WT Δcbp	P_{chb}-GFP @ lacZ, KanR; P_{chiS}-ChiS WT @ VCA0692, TmR; ΔchiS/cbp::CarbR
This study (CAK 1031/ SAD 2676)	Fig. 1A D772A cbp+	P_{chb}-GFP @ lacZ, KanR; P_{chiS}-ChiS D772A @ VCA0692, TmR; ΔchiS::CarbR
This study (CAK 1032/ SAD 2677)	Fig. 1A D772A Δcbp	P_{chb}-GFP @ lacZ, KanR; P_{chiS}-ChiS D772A @ VCA0692, TmR; ΔchiS/cbp::CarbR
This study (CAK 1264/ SAD 2678)	Fig. 1A WT cbp+	P_{chb}-GFP @ lacZ, KanR; P_{chiS}-ChiS @ VCA0692, TmR; ΔchiS::CarbR
This study (CAK 1265/ SAD 2679)	Fig. 1A T473A D772A cbp+	P_{chb}-GFP @ lacZ, KanR; P_{chiS}-ChiS T473A D772A @ VCA0692, TmR; ΔchiS::CarbR
This study (CAK 1266/ SAD 2680)	Fig. 1A H469A cbp+	P_{chb}-GFP @ lacZ, KanR; P_{chiS}-ChiS H469A @ VCA0692, TmR; ΔchiS::CarbR
This study (CAK 1267/ SAD 2681)	Fig. 1A H469A Δcbp	P_{chb}-GFP @ lacZ, KanR; P_{chiS}-ChiS H469A @ VCA0692, TmR; ΔchiS/cbp::CarbR
This study (CAK 1268/ SAD 2682)	Fig. 1A H469A T473A cbp+	P_{chb}-GFP @ lacZ, KanR; P_{chiS}-ChiS H469A T473A @ VCA0692, TmR; ΔchiS::CarbR

This study (CAK 1269/ SAD 2683)	Fig. 1A H469A T473A ∆cbp	P_{chb}-GFP @ lacZ, KanR; P_{chiS}-ChiS H469A T473A @ VCA0692, TmR; ∆chiS/cbp::CarbR
This study (CAK 1272/ SAD 2684)	Fig. 1A H469A D772A cbp+	P_{chb}-GFP @ lacZ, KanR; P_{chiS}-ChiS H469A D772A @ VCA0692, TmR; ∆chiS::CarbR
This study (CAK 1273/ SAD 2685)	Fig. 1A H469A D772A ∆cbp	P_{chb}-GFP @ lacZ, KanR; P_{chiS}-ChiS H469A D772A @ VCA0692, TmR; ∆chiS/cbp::CarbR
This study (CAK 1356/ SAD 2686)	Fig. 1A ∆chiS ∆cbp	P_{chb}-GFP @ lacZ, KanR; ∆chiS/cbp::CarbR
This study (CAK 1376/ SAD 2687)	Fig. 1B, S2, & S4 ∆chiS	∆VC0995::CmR; ∆chiS::CarbR
This study (CAK 1377/ SAD 2688)	Fig. 1B D772E	P_{chb}-GFP @ lacZ, KanR; ∆chiS::CarbR; P_{chiS}-ChiS D772E @ VCA0692, TmR; ∆VC0995::CmR
This study (CAK 1378/ SAD 2689)	Fig. 1B, S2, & S4 T473A	P_{chb}-GFP @ lacZ, KanR; ∆chiS::CarbR; P_{chiS}-ChiS T473A @ VCA0692, TmR; ∆VC0995::CmR
This study (CAK 1379/ SAD 2690)	Fig. S2 & S4 D772A	P_{chb}-GFP @ lacZ, KanR; ∆chiS::CarbR; P_{chiS}-ChiS D772A @ VCA0692, TmR; ∆VC0995::CmR
This study (CAK 1380/ SAD 2691)	Fig. 1B, S2, & S4 WT	P_{chb}-GFP @ lacZ, KanR; P_{chiS}-ChiS @ VCA0692, TmR; ∆chiS::CarbR; ∆VC0995::CmR
This study (CAK 1381/ SAD 2692)	Fig. S2 & S4 T473A D772A	P_{chb}-GFP @ lacZ, KanR; P_{chiS}-ChiS T473A D772A @ VCA0692, TmR; ∆chiS::CarbR; ∆VC0995::CmR
This study (CAK 1382/ SAD 2693)	Fig. S2 & S4 H469A	P_{chb}-GFP @ lacZ, KanR; P_{chiS}-ChiS H469A @ VCA0692, TmR; ∆chiS::CarbR; ∆VC0995::CmR
This study (CAK 1383/ SAD 2694)	Fig. S2 & S4 T473A H469A	P_{chb}-GFP @ lacZ, KanR; P_{chiS}-ChiS H469A T473A @ VCA0692, TmR; ∆chiS::CarbR; ∆VC0995::CmR
This study (CAK 1385/ SAD 2695)	Fig. S2 & S4 H469A D772A	P_{chb}-GFP @ lacZ, KanR; P_{chiS}-ChiS H469A D772A @ VCA0692, TmR; ∆chiS::CarbR; ∆VC0995::CmR
(48) (SAD 720)	Parent strain for E. coli P_{chb}-*lacZ* strain	*E. coli* MG1655 WT
This study (CAK 1027/ SAD2743)	*E. coli* MG1655 P_{chb}-*lacZ*, KanR @ *lacZ* background for harboring various vectors	*E. coli* MG1655 P_{chb}-*lacZ*, KanR @ *lacZ*
This study	Fig. 2A ChiS WT for Miller	*E. coli* MG1655 P_{chb}-lacZ @ lacZ, KanR;

(CAK 1033/ SAD 2696)	Assay	pMMB67EH+riboswitchE with ChiS, CarbR
This study (CAK 1037/ SAD 2697)	Fig. 2A Empty vector	*E. coli* MG1655 P_{chb}-lacZ @ lacZ, KanR; pMMB67EH+riboswitchE Empty Vector, CarbR
This study (CAK 1410/ SAD 2698)	Fig. 2A ChiS D772E for Miller Assay	*E. coli* MG1655 P_{chb}-lacZ @ lacZ, KanR; pMMB67EH+riboswitchE with ChiS D772E, CarbR
This study (CAK 1408/ SAD 2699)	Fig. 2A ChiS WT for ChIP	*E. coli* MG1655 P_{chb}-lacZ @ lacZ, KanR; pMMB67EH+riboswitchE with ChiS internal 1x FLAG @ E566, CarbR
This study (CAK 1409/ SAD 2700)	Fig. 2A ChiS D772E for ChIP	*E. coli* MG1655 P_{chb}-lacZ @ lacZ, KanR; pMMB67EH+riboswitchE with ChiS D772E internal 1x FLAG @ E566, CarbR
This study (CAK 1335/ SAD 2701)	Fig. 2B & S5 ChiS-FLAG WT cyto cbp+	P_{chb}-GFP @ lacZ, KanR; P_{chiS}-ChiS internal single FLAG after E566 @ VCA0692 TmR; ΔchiS::CarbR
This study (CAK 1346/ SAD 2702)	Fig. 2B & S5 ChiS-FLAG D772E cyto Δcbp	P_{chb}-GFP @ lacZ, KanR; P_{chiS}-ChiS D772E internal single FLAG after E566 @ VCA0692 TmR; ΔchiS/cbp::CarbR
This study (CAK 1362/ SAD 2703)	Fig. 2B Ptac ChiS-FLAG WT cyto Δcbp	P_{chb}-GFP @ lacZ, KanR; P_{tac}-ChiS internal 1x FLAG @ E566 @ VCA0692, TmR; ΔchiS/cbp::CarbR
This study (CAK 1363/ SAD 2704)	Fig. 2B Ptac ChiS-FLAG D772E cyto Δcbp	P_{chb}-GFP @ lacZ, KanR; P_{tac}-ChiS D772E internal 1x FLAG @ E566 @ VCA0692, TmR; ΔchiS/cbp::CarbR
This study (TND 1795/ SAD 2705)	Fig. 2B ChiS-FLAG WT peri Δcbp	P_{chb}-GFP @ lacZ, KanR; P_{chiS}-ChiS internal single FLAG after T287 @ VCA0692 TmR; ΔchiS/cbp::CarbR
This study (TND 1801/ SAD 2706)	Fig. 2B & S5 ChiS-FLAG WT cyto Δcbp	P_{chb}-GFP @ lacZ, KanR; P_{chiS}-ChiS internal single FLAG after E566 @ VCA0692 TmR; ΔchiS/cbp::CarbR
This study (CAK 1350/ SAD 2707)	Fig. 3B BS 1 Mutate	P_{chb} ChiS BS 1 transition mutated @ native; ΔVC1807::SpecR; ΔVC0995::CmR
This study (CAK 1351/ SAD 2708)	Fig. 3B BS 2 Mutate	P_{chb} ChiS BS 2 transition mutated @ native; ΔVC1807::SpecR; ΔVC0995::CmR
This study (CAK 1352/ SAD 2709)	Fig. 3B BS 1 & 2 Mutate	P_{chb} ChiS BS 1 & 2 transition mutated @ native; ΔVC1807::SpecR; ΔVC0995::CmR
This study (CAK 1376/ SAD 2710)	Fig. 3B ΔchiS	ΔVC0995::CmR; ΔchiS::CarbR
This study (CAK 1358/	Fig. 3B WT	ΔVC0995::CmR

SAD 2711)		
(7) (SAD 590/ CAK 007)	Fig. 3C & 4A WT cbp+	P_{chb}-GFP @ lacZ, KanR
(7) (SAD 1390/ CAK 009)	Fig. 3C & 4A WT ∆cbp	P_{chb}-GFP @ lacZ, KanR; ∆cbp::SpecR
This study (CAK 1235/ SAD 2712)	Fig. 3C BS 1 mutate cbp+	P_{chb} ChiS BS 1 transition mutate-GFP @ lacZ, KanR
This study (CAK 1236/ SAD 2713)	Fig. 3C BS 1 mutate ∆cbp	P_{chb} ChiS BS 2 transition mutate-GFP @ lacZ, KanR
This study (CAK 1241/ SAD 2714)	Fig. 3C BS 2 mutate cbp+	P_{chb} ChiS BS 1 transition mutate-GFP @ lacZ, KanR; ∆cbp::SpecR
This study (CAK 1242/ SAD 2715)	Fig. 3C BS 2 mutate ∆cbp	P_{chb} ChiS BS 2 transition mutate-GFP @ lacZ, KanR; ∆cbp::SpecR
This study (CAK 1279/ SAD 2716)	Fig. 3C BS 1 & 2 mutate cbp+	P_{chb} ChiS BS 1 & 2 transition mutate-GFP @ lacZ, KanR
This study (CAK 1290/ SAD 2717)	Fig. 3C BS 1 & 2 mutate ∆cbp	P_{chb} ChiS BS 1 & 2 transition mutate-GFP @ lacZ, KanR; ∆cbp::SpecR
This study (CAK 1293/ SAD 2718)	Fig. 4A Region A +5 ∆cbp	P_{chb} insert 5 bp between ChiS BS 2 and -35-GFP @ lacZ, KanR; ∆cbp::SpecR
This study (CAK 1294/ SAD 2719)	Fig. 4A Region A +10 ∆cbp	P_{chb} insert 10 bp between ChiS BS 2 and -35-GFP @ lacZ, KanR; ∆cbp::SpecR
This study (CAK 1411/ SAD 2720)	Fig. 4A Region B +5 ∆cbp	P_{chb} insert 5 bp upstream ChiS BS 1-GFP @ lacZ, KanR; ∆cbp::SpecR
This study (CAK 1412/ SAD 2721)	Fig. 4A Region B +10 ∆cbp	P_{chb} insert 10 bp upstream ChiS BS 1-GFP @ lacZ, KanR; ∆cbp::SpecR
This study (CAK 1413/ SAD 2722)	Fig. 4A Region B -5 ∆cbp	P_{chb} delete 5 bp upstream ChiS BS 1-GFP @ lacZ, KanR; ∆cbp::SpecR
This study (CAK 1414/ SAD 2723)	Fig. 4A Region B -10 ∆cbp	P_{chb} delete 10 bp upstream ChiS BS 1-GFP @ lacZ, KanR; ∆cbp::SpecR
This study (CAK 1430/ SAD 2724)	Fig. 4A Region A +5 Region B +5 ∆cbp	P_{chb} insert 5 bp upstream ChiS BS 1 and insert 5 bp bewteen ChiS BS 2 and -35-GFP @ lacZ, KanR; ∆cbp::SpecR

This study (CAK 1432/ SAD 2725)	Fig. 4A Region A +5 Region B -5 ∆cbp	P_{chb} delete 5 bp upstream ChiS BS 1 and insert 5 bp bewteen ChiS BS 2 and -35-GFP @ lacZ, KanR; ∆cbp::SpecR
This study (CAK 1341/ SAD 2726)	Fig. S5 T473A ∆cbp	P_{chb}-GFP @ lacZ, KanR; P_{chiS}-ChiS T473A internal single FLAG after E566 @ VCA0692 TmR; ∆chiS/cbp::CarbR
This study (CAK 1364/ SAD 2727)	Fig. S5 H469A ∆cbp	P_{chb}-GFP @ lacZ, KanR; P_{chiS}-ChiS H469A internal 1x FLAG @ E566 @ VCA0962, TmR; ∆chiS/cbp::CarbR
This study (CAK 1365/ SAD 2728)	Fig. S5 H469A T473A ∆cbp	P_{chb}-GFP @ lacZ, KanR; P_{chiS}-ChiS H469A T473A internal 1x FLAG @ E566 @ VCA0692, TmR; ∆chiS/cbp::CarbR
This study (CAK 1367/ SAD 2729)	Fig. S5 H469A D772A ∆cbp	P_{chb}-GFP @ lacZ, KanR; P_{chiS}-ChiS H469A D772A internal 1x FLAG @ E566 @ VCA0692, TmR; ∆chiS/cbp::CarbR
This study (CAK 1368/ SAD 2730)	Fig. S5 D772A ∆cbp	P_{chb}-GFP @ lacZ, KanR; P_{chiS}-ChiS D772A internal 1x FLAG @ E566 @ VCA0692, TmR; ∆chiS/cbp::CarbR
This study (CAK 1415/ SAD 2731)	Fig. S5 T473A D772A ∆cbp	P_{chb}-GFP @ lacZ, KanR; P_{chiS}-ChiS T473A D772A internal 1x FLAG @ E566 @ VCA0692, TmR; ∆chiS/cbp::CarbR
This study (CAK 1131/ SAD 2732)	Fig. S9 ChiS 377-1129	P_{chb}-GFP @ lacZ, KanR; P_{tac}-3x FLAG ChiS cytoplasmic @ VCA0692, TmR; ∆chiS::CarbR
This study (CAK 1133/ SAD 2733)	Fig. S9 ChiS 725-1129	P_{chb}-GFP @ lacZ, KanR; P_{tac}-3x FLAG $ChiS^{Rec\text{-}C}$ @ VCA0692, TmR; ∆chiS::CarbR
This study (CAK 1258/ SAD 2734)	Fig. S9 ChiS 1024-1129	P_{chb}-GFP @ lacZ, KanR; P_{tac}-3x FLAG last 99 amino acids of ChiS @ VCA0692, TmR; ∆chiS::CarbR
This study (CAK 1322/ SAD 2735)	Fig. S9 ChiS 1031-1129	P_{chb}-GFP @ lacZ, KanR; P_{tac}-3x FLAG ChiS last 106 amino acids @ VCA0692, TmR; ∆chiS::CarbR
This study (CAK 1434/ SAD 2736)	Fig. S9 ChiS 1-1023	P_{chb}-GFP @ lacZ, KanR; P_{chiS}-ChiS 1x FLAG @ E566 ∆last 106 amino acids @ VCA0692, TmR; ∆chiS/cbp::CarbR
(8)	Fig. S6 Empty vector, beta-galactosidase bar	*E. coli* DH1 Δ*lacIZYA*::FRT Δ*phoA*::FRT::*kan*::FRT harboring pMW119 '*lacZ*
This study	Fig. S6 $ChiS^{1\text{-}2}$, beta-galactosidase bar	*E. coli* DH1 Δ*lacIZYA*::FRT Δ*phoA*::FRT::*kan*::FRT harboring pMW-SY*lacZ* P*chiS*::*chiS*' (encoding 1 to 2 aa)
This study	Fig. S6 $ChiS^{1\text{-}52}$, beta-galactosidase bar	*E. coli* DH1 Δ*lacIZYA*::FRT Δ*phoA*::FRT::*kan*::FRT harboring pMW-SY*lacZ* P*chiS*::*chiS*' (encoding 1 to

		52 aa)
This study	Fig. S6 ChiS$^{1-452}$, beta-galactosidase bar	*E. coli* DH1 Δ*lacIZYA*::FRT Δ*phoA*::FRT::*kan*::FRT harboring pMW-SY*lacZ* P*chiS*::*chiS*' (encoding 1 to 452 aa)
This study	Fig. S6 ChiS$^{1-1129}$, beta-galactosidase bar	*E. coli* DH1 Δ*lacIZYA*::FRT Δ*phoA*::FRT::*kan*::FRT harboring pMW-SY*lacZ* P*chiS*::*chiS* (encoding 1 to 1129 aa)
(8)	Fig. S6 Empty vector, alkaline phosphatase bar	*E. coli* DH1 Δ*lacIZYA*::FRT Δ*phoA*::FRT::*kan*::FRT harboring pMW119 '*phoA*
This study	Fig. S6 ChiS$^{1-2}$, alkaline phosphatase bar	*E. coli* DH1 Δ*lacIZYA*::FRT Δ*phoA*::FRT::*kan*::FRT harboring pMW-SY*phoA* P*chiS*::*chiS*' (encoding 1 to 2 aa)
This study	Fig. S6 ChiS$^{1-52}$, alkaline phosphatase bar	*E. coli* DH1 Δ*lacIZYA*::FRT Δ*phoA*::FRT::*kan*::FRT harboring pMW-SY*phoA* P*chiS*::*chiS*' (encoding 1 to 52 aa)
This study	Fig. S6 ChiS$^{1-452}$, alkaline phosphatase bar	*E. coli* DH1 Δ*lacIZYA*::FRT Δ*phoA*::FRT::*kan*::FRT harboring pMW-SY*phoA* P*chiS*::*chiS*' (encoding 1 to 452 aa)
This study	Fig. S6 ChiS$^{1-1129}$, alkaline phosphatase bar	*E. coli* DH1 Δ*lacIZYA*::FRT Δ*phoA*::FRT::*kan*::FRT harboring pMW-SY*phoA* P*chiS*::*chiS* (encoding 1 to 1129 aa)

Strains used for protein purification

Strain	Genotype
This study (CAK 1185/ SAD 2737)	*E. coli* BL21 harboring pHisTev ChiS^{Rec-C}, CarbR
This study (CAK 1276/ SAD 2738)	*E. coli* BL21 harboring pMAL-C2-Tev ChiS cytoplasmic, CarbR
This study (CAK 1303/ SAD 2739)	*E. coli* BL21 harboring pMAL-C2-Tev ChiS cytoplasmic H469A, CarbR
This study (CAK 1304/ SAD 2740)	*E. coli* BL21 harboring pMAL-C2-Tev ChiS cytoplasmic T473A, CarbR

Table S3. *Primers used in this study.*

Primers for SOE deletions		
Primer	**Sequence**	**Description**
BBC 742	attccggggatccgtcgacCTGCAGTTCagaagcagctccagcctaca	MiniFRT F
BBC 743	tgtaggctggagctgcttctGAACTGCAGgtcgacggatcccccggaat	MiniFRT R
ABD 123	ATTCCGGGGATCCGTCGAC	Kan^R, $Spec^R$, $Carb^R$, Cm^R or Tm^R cassette F
ABD 124	TGTAGGCTGGAGCTGCTTC	Kan^R, $Spec^R$, $Carb^R$, Cm^R or Tm^R cassette R
ABD 767	TTAATTTGGATCCCTGCGACACTC	ΔchiS F1 for Up arm
ABD 768	gtcgacggatccccggaatCAAAAAACGTGAGGAGAATGCC	ΔchiS R1 for Up arm
ABD 769	gaagcagctccagcctacaTTCTTGAGCATTGCAAAGAAGC	ΔchiS F2 for Down arm
ABD 770	CTGGAACGAATGAAGAAGTCCAG	ΔchiS R2 for Down arm
ABD 796	TTAGAATCTGCGCCAGAAGCG	Δcbp F1 for Up arm
ABD 797	gtcgacggatccccggaatCATAGCTGTTCCTTACTAGTTGC	Δcbp R1 for Up arm
ABD 798	gaagcagctccagcctacaGTACTGGATCTGAAACCAGTTAAG	Δcbp F2 for Down arm
ABD 799	GTATTGCGGAATGACCAGCATG	Δcbp R2 for Down arm
ABD 927	GCAGAGAAAGGGTATCATTACTGG	ΔVC0995 F1 for Up arm
ABD 928	GcTAATTCAGTTTAAGCGGCCATCTTAAGTTCCCCCTATAGGATTTTTG	ΔVC0995 R1 for Up arm
ABD 929	ATGGCCGCTTAAACTGAATTAgCACATCAGGTGCTTTAGGCCAATTTG	ΔVC0995 F2 for Down arm
ABD 930	TACTCTCGTTTTTCGGCTTACTC	ΔVC0995 R2 for Down arm
BBC 717	AAATAGATTTGGTGACTTTACCTCC	ΔVC1807 F1 for Up arm
ABD 340	gtcgacggatccccggaatACGTTTCATTAGTCACCTCTATTGTTAACTTGTTC	ΔVC1807 R1 for Up arm
ABD 341	gaagcagctccagcctacaTAGTCGAAAATAAAAAAAAGAGGCTCGCCTC	ΔVC1807 F2 for Down arm
BBC 718	CTTTACGCCTGATTGTCTACAC	ΔVC1807 R2 for Down arm
ABD 725	GAAGCAGCTCCAGCCTACA	Detect F for all deletions
CKP 001	cccgggatcctgtgtgaaattgCTTATTTGGCCTTGTTTGATAATG	ΔchiS detect R
BBC 082	gtcgacggatccccggaatCATAACTTACACCTTACTCACCCAG	Δcbp detect R
ABD 971	CAACTAGGGTTTTCGCTAGAGC	ΔVC0995 detect R
BBC 030	ACCAAACAATAAACGAGTAATGC	ΔVC1807 detect R

Primers for P_{chb} Mutations		
Primer	**Sequence**	**Description**
CKP 627	CAGAAGGTATTTTGAtacTAATGACGTAGG	ChiS BS 1 mutate F2
CKP 628	CCTACGTCATTAgtaTCAAAATACCTTCTG	ChiS BS 1 mutate R1
CKP 640	GGTTTTGAtacTTTTAACGGGAATTGCAAT	ChiS BS 2 mutate F2
CKP 641	ATTGCAATTCCCGTTAAAAgtaTCAAAACC	ChiS BS 2 mutate R1
CKP 658	CACACATCAGAAGGTATTTTGAtac	ChiS BS 1 mutate detect F
CKP 659	GTAGGGCATCTAGGTTTTGAtac	ChiS BS 2 mutate detect F
BBC 919	GGTTCATAGATAAAGTCGGTGGTTG	ChiS BS mutate detect R
CKP 678	GTTTTTAACGGGAATtttttTGCAATTGATAAATTTCTTGGC	Region A +5 bp F2
CKP 679	AATTTATCAATTGCAaaaaaATTCCCGTTAAAAACGTCAAAACC	Region A +5 bp R1
CKP 680	GTTTTTAACGGGAATtttttttttTGCAATTGATAAATTTCTTGGC	Region A +10 bp F2
CKP 681	AATTTATCAATTGCAaaaaaaaaaaATTCCCGTTAAAAACGTCAAAACC	Region A +10 bp R1
CKP 738	CACACATCAGAAGGTtttttATTTTGACGTTAATGACGTAG	Region B +5 bp F2
CKP 739	ATTAACGTCAAAATaaaaaACCTTCTGATGTGTGATTTTTG	Region B +5 bp R1
CKP 740	CACACATCAGAAGGTttttttttttATTTTGACGTTAATGACGTAG	Region B +10 bp F2
CKP 741	ATTAACGTCAAAATaaaaaaaaaaACCTTCTGATGTGTGATTTTTG	Region B +10 bp R1
CKP 742	CACACATCAGATTTTGACGTTAATGACGTAG	Region B -5 bp F2
CKP 743	ATTAACGTCAAAATCTGATGTGTGATTTTTG	Region B -5 bp R1
CKP 744	ACAAAAATCACACATTTTGACGTTAATGACGTAGG	Region B -10 bp F2
CKP 745	TCATTAACGTCAAAATGTGTGATTTTTGTACAAAAAC	Region B -10 bp R1
Primers for qPCR		
Primer	**Sequence**	**Description**
BBC 989	GCATCTAGGTTTTGACGTTTTTAACG	Pchb amplify F
BBC 990	AACACTCTCCAAGACCTACCTC	Pchb amplify R
ABD 132	CTGTCTCAAGCCGGTTACAA	V. cholerae rpoB amplify F
ABD 133	TTTCTACCAGTGCAGAGATGC	V. cholerae rpoB amplify R
CKP 575	TCTCCTTTCTATCCAGCTTG	E. coli rpoB amplify F
CKP 576	CCAAGGCGGTAGCTGACG	E. coli rpoB amplify R
Primers for EMSAs		

Primer	Sequence	Description
BBC 744	cagcttcgcgtcctcggtaCGCAAATATAACTCAGGCAAAG	P_{chb} F
CKP 072	cccgggatcctgtgtgaaattgCTTTGGCAGGAGTAAGAAAACACCTAG	P_{chb} R
CKP 250	CTCAACGTTTGCCTTATC	$P_{VCA0053}$ F
CKP 251	GGATCCTGTTGGCTCAAG	$P_{VCA0053}$ R
CKP 327	CAGAAGGTATTTTGACGTTAATGACGTAGG	Segment 1 30bp F
CKP 328	CCTACGTCATTAACGTCAAAATACCTTCTG	Segment 1 30bp R
CKP 329	CGTTAATGACGTAGGGCATCTAGGTTTTGA	Segment 2 30bp F
CKP 330	TCAAAACCTAGATGCCCTACGTCATTAACG	Segment 2 30bp R
CKP 331	GACGTAGGGCATCTAGGTTTTGACGTTTTT	Segment 3 30bp F
CKP 332	AAAAACGTCAAAACCTAGATGCCCTACGTC	Segment 3 30bp R
CKP 631	GGTTTTGACGTTTTTAACGGGAATTGCAAT	Segment 4 30bp F
CKP 632	ATTGCAATTCCCGTTAAAAACGTCAAAACC	Segment 4 30bp R
CKP 633	AACGGGAATTGCAATTGATAAATTTCTTGG	Segment 5 30bp F
CKP 634	CCAAGAAATTTATCAATTGCAATTCCCGTT	Segment 5 30bp R
CKP 635	TGATAAATTTCTTGGCTAGGTGTTTTCTTA	Segment 6 30bp F
CKP 636	TAAGAAAACACCTAGCCAAGAAATTTATCA	Segment 6 30bp R
CKP 637	TGGCTAGGTGTTTTCTTACTCCTGCCAAAG	Segment 7 30bp F
CKP 638	CTTTGGCAGGAGTAAGAAAACACCTAGCCA	Segment 7 30bp R
CKP 642	GGTATTTTGACGTTAATGACGTAGGGCATCTAGGTTTTGACGTTTTTAACGGGAATTGCA	Pchb 60 bp WT F
CKP 643	TGCAATTCCCGTTAAAAACGTCAAAACCTAGATGCCCTACGTCATTAACGTCAAAATACC	Pchb 60 bp WT R
CKP 644	GGTATTTTGAtacTAATGACGTAGGGCATCTAGGTTTTGACGTTTTTAACGGGAATTGCA	Pchb 60 bp ChiS BS 1 Mutate F
CKP 645	TGCAATTCCCGTTAAAAACGTCAAAACCTAGATGCCCTACGTCATTAgtaTCAAAATACC	Pchb 60 bp ChiS BS 1 Mutate R
CKP 646	GGTATTTTGACGTTAATGACGTAGGGCATCTAGGTTTTGAtacTTTTAACGGGAATTGCA	Pchb 60 bp ChiS BS 2 Mutate F
CKP 647	TGCAATTCCCGTTAAAAgtaTCAAAACCTAGATGCCCTACGTCATTAACGTCAAAATACC	Pchb 60 bp ChiS BS 2 Mutate R
CKP 648	GGTATTTTGAtacTAATGACGTAGGGCATCTAGGTTTTGAtacTTTTAACGGGAATTGCA	Pchb 60 bp ChiS BS 1 & 2 Mutate F
CKP 649	TGCAATTCCCGTTAAAAgtaTCAAAACCTAGATGCCCTACGTCATTAgtaTCAAAATACC	Pchb 60 bp ChiS BS 1 & 2 Mutate R
Primers for Reporter Constructs		
Primer	**Sequence**	**Description**
ABD 332	GGCTGAACGTGGTTGTCGAAAATGAC	Δ*lacZ* F1 (Up Arm)
BBC 219	GTTTATTTTTGTCGACTGTACAGCGTTTAAATAGAGGTCGATATTGACCC	Δ*lacZ* R1 (Up Arm)
BBC 218	CGCTGTACAGTCGACAAAAATAAAC	Kan^R F (Middle Arm)
BBC 262	TACCGAGGACGCGAAGCTG	Kan^R R (Middle Arm)
BBC 266	CAGCTTCGCGTCCTCGGTAGAATAAAGCAA	P_{chb} F (Middle Arm)

	TCCGCAAGCG	
BBC 267	CCCGGGATCCTGTGTGAAATTGAGTTGCTTTCATTTCACTAATGG	P_{chb} R (Middle Arm)
BBC 252	CAATTTCACACAGGATCCCGGGAGGAGGTAACGTAATGCGTAAAGGAGAAGAAC	GFP F (Middle Arm)
BBC 254	tgtaggctggagctgcttcTTAGTTGTATAGTTCATCCATGCC	GFP R (Middle Arm)
ABD 255	gaagcagctccagcctacaCCACAATAAGCCAGAGAGCCTTAAG	Δ*lacZ* F2 (Down Arm)
ABD 256	CCCAAATACGGCAACTTGGCG	Δ*lacZ* R2 (Down Arm)
BBC 1311	AAGAAGGGGTTGAATCGCAGGCTATTCTGGTGGCCGGAAGGCGAAGCGGCATGCATTTACGTTGACGCTGTACAGTCGACAAAAATAAAC	Amplify KanR-Pchb for E. coli lacZ reporter F
BBC 1313	TTCCCAGTCACGACGTTGTAAAACGACGGCCAGTGAATCCGTAATCATGGTCATAGCTGTacctcctAGTTGCTTTCATTTCACTAATGG	Amplify KanR-Pchb for E. coli lacZ reporter R
Primers for ChiS constructs		
Primer	**Sequence**	**Description**
BBC 832	GCTTTTTGCTACAACGACCG	VCA0692 Tm^R F1 for Up arm
BBC 647	tttttctatttctgaatcgattcatacgaCTCATTAGGCACCCCAGGC	VCA0692 Tm^R R1 for P_{chiS} Up arm
BBC 244	CCCGGGATCCTGTGTGAAATTGTTATCCGC	VCA0692 TmR R1 for P_{tac} Up arm
BBC 2667	tccaccacttccacctgcCATTACGTTACCTCCTCCCG	VCA0692 TmR R1 for P_{tac}-3x FLAG constructs for Up arm
BBC 1889	tcgtatgaatcgattcagaaatagaaaaaTTTGCCGCTTTTAACGTAAATCAG	P_{chiS}-ChiS F for Middle arm
BBC 1236	caatttcacacaggatcccgggAGGAGGTaacgtaATGTTTAGGTTCTATCGAAAACAA	P_{tac}-ChiS full F for Middle arm
CKP 589	gcaggtggagcaggtggaAATTTCATTACCTCACCGCTTTTGAAGC	P_{tac}-3x FLAG ChiS cytoplasmic F for Middle arm
CKP 590	gcaggtggagcaggtggaTTGGTCGCCGATGATGAACC	P_{tac}-3x FLAG $ChiS^{Rec\text{-}C}$ F for Middle arm
CKP 710	gcaggtggagcaggtggaTCGAAACAAGATTTGATGCG	P_{tac}-3x FLAG ChiS last 106 amino acids F for Middle arm
CKP 669	gcaggtggagcaggtggaGCCGTGTTAGTCGAAGCCATG	P_{tac}-3x FLAG ChiS last 99 amino acids F for Middle arm
BBC 577	tgtaggctggagctgcttcTTATTCACTGGTCAGGAGTTTTTGC	ChiS R for Middle arm
BBC 830	gaagcagctccagcctacaGTTGAGTTGGATGCAG	VCA0692 F2 for Down

	CACC	arm
BBC 834	CACAATTTCTCGCTTAAAATGTCC	VCA0692 R2 for Down arm
DOG 0718	gcaggtggagcaggtggaCAACCGGTCTGGGTTTCTG	ChiS internal tag after E566 F
DOG 0717	tccaccacttccacctgcTTCTGAGACTTGATTAATAATGCGCAG	ChiS internal tag after E566 R
DOG 0714	gcaggtggagcaggtggaTCCGCCGAAATTGCGGTTG	ChiS internal tag after T287 F
DOG 0713	tccaccacttccacctgcAGTTAAGGTTCTTGAGCGGTG	ChiS internal tag after T287 R
BBC 2274	gcaggtggaagtggtggagattataaggatgacgatgacaaagcaggtggagcaggtgga	1x FLAG Mix for SOE F
BBC 2275	tccacctgctccacctgctttgtcatcgtcatccttataatctccaccacttccacctgc	1x FLAG Mix for SOE R
CKP 729	GATAAAGCCTCGGGCGAGTATCAATAAgaagcagctccagcctaca	ChiS ∆last 106 F
CKP 728	TTGATACTCGCCCGAGGCTTTATC	ChiS ∆last 106 R
BBC 367	GTTCCTCGCGACCACATCAgcaGAATTACGCACCCCATTGC	H469A F
BBC 366	GCAATGGGGTGCGTAATTCtgcTGATGTGGTCGCGAGGAAC	H469A R
BBC 372	CCTCGCGACCACATCAgca	H469A detect F
CKP 228	CACATGAATTACGCgCCCCATTGCATGGCATGATTG	T473A F
CKP 229	GCCATGCAATGGGGcGCGTAATTCATGTGATGTGG	T473A R
CKP 230	CACATCACATGAATTACGtg	T473A detect F
CKP 030	GTGTTACTCGcCATCATGATG	D772A F
CKP 031	CATCATGATGgCGAGTAACAC	D772A R
CKP 034	GAATTGGTGTTACTCac	D772A detect F
CKP 534	ATTGGTGTTACTCGAaATCATGATGCCAGGCATGAG	D772E F
CKP 535	GCCTGGCATCATGATtTCGAGTAACACCAATTCAGG	D772E R
CKP 536	CTGAATTGGTGTTACTCGga	D772E detect F
CKP 676	CCTCGCGACCACATCAgcaGAATTACGC	H469A T473A F
CKP 677	TAATTCtgcTGATGTGGTCGCGAGGAAC	H469A T473A R
CKP 024	cttcttcgctcgccagaggGCGTTGAGGATCCGCAGAAA	H469A and T473A detect R
CKP 035	GCCGCTTCGTTAGCAAAACG	D772 mutants detect R
Primers for vector constructs		
Primer	**Sequence**	**Description**
BBC 2424	gGATCCTCTAGAGTCGACCTGCAGGCAAGCTTGGCACTGG	pMAL-C2-TEV amplify for Fast Clone F

BBC 2423	atggccctgaaaatacaggttttcaAATTCTGAAATCCTTCCCTC	pMAL-C2-TEV amplify for Fast Clone R
CKP 655	gaaaacctgtattttcagggccatAATTTCATTACCTCACCGCTTTTG	ChiS pMAL insert amplify F
CKP 657	aagcttgcctgcaggtcgactctagaggatccTTATTCACTGGTCAGGAGTTTTTG	ChiS pMAL insert amplify R
BBC 2138	gctgttttggcggatgagag	pMMB + riboE amplify for Fast Clone F
BBC 2137	CTTGTTGTTACCTCCTTAGCAGG	pMMB + riboE amplify for Fast Clone R
CKP 574	cctgctaaggaggtaacaacaagATGTTTAGGTTCTATCGAAAAC	ChiS pMMB + riboE insert amplify F
BBC 2136	ctctcatccgccaaaacagcTTATTCACTGGTCAGGAGTTTTTGC	ChiS pMMB + riboE insert amplify R
CKP 090	cggatccGGCTGCTAACAAAG	pHisTev amplify for Fast Clone F
BBC 2359	atggccctgaaaatacaggttttctatATGGCTGCCGCGCGGCACC	pHisTev amplify for Fast Clone R
CKP 616	CATatagaaaacctgtattttcagggccatTTGGTCGCCGATGATGAACC	ChiS Rec + C-terminus pHisTev insert amplify F
CKP 484	CCTTTCGGGCTTTGTTAGCAGCCggatccgTTATTCACTGGTCAGGAGTTTTTGC	ChiS Rec + C-terminus pHisTev insert amplify R
BBC 081	AAGCAAGTTCACGTTTGCCG	ChiS detect in vector F
BBC 185	GCGTTCTGATTTAATCTGTATCAGG	pMMB67EH detect R
BBC 798	CCTCAAGACCCGTTTAGAG	pHisTev detect R
BBC 2464	CGCCAGGGTTTTCCCAGTC	pMAL-C2-TEV detect R
CHISf4S	GGGGGTCGAC ACGTAAATCA GCCTCAAAAG	F for chiS' phoA and lacZ fusions
CHISr3X	GGGGTCTAGA AAACATAATT AAGGTGTTAC	R for chiS' (encoding 1 to 2 aa) phoA and lacZ fusions
CHISr4X	GGGGTCTAGA GAGGTAAGAA GTGCTCTGCT	R for chiS' (encoding 1 to 52 aa) phoA and lacZ fusions
CHISr5X	GGGGTCTAGA CTCATCGTTT TGCTTACGAA	R for chiS' (encoding 1 to 452 aa) phoA and lacZ fusions
CHISr6X	GGGGTCTAGA TTCACTGGTC AGGAGTTTTT	R for chiS' (encoding 1 to 1129 aa) phoA and lacZ fusions